



**POLITECNICO
DI TORINO**

Master of Science in Civil Engineering

Master's Thesis

**Mechanical behaviour and durability of self-healing
cementitious systems: image analysis of healing
agent diffusion correlated with mechanical and
durability parameters**

Advisors

Prof. Paola Antonaci

Eng. Giovanni Anglani

Candidate

Nicole Priante

July 2020

Abstract

Concrete is the most used material in the field of Civil Engineering, due to the considerable flexibility that it offers in design, and also due to its low cost. On the other hand, because of its reduced tensile strength, it is also one of the most prone to cracking materials. For this reason, solutions for damage management have been developed in recent years. However, current researches point to sustainable treatments, both in ecological and economic terms. The idea is to enhance the service life of structures through the improvement of the physiological self-repairing properties of concrete. Therefore, self-healing cement-based materials have been targeted, through the use of different strategies including nonencapsulated and encapsulated technologies, to be embedded inside the matrix during the casting phase. The former include all methods that stimulate the main mechanisms producing autogenous self-healing of cementitious material, in form of mineral additions or crystalline admixtures; the latter allow the direct internal availability of healing agent at the location of damage through the storage of the sealant inside micro or macrocapsules. It is evident that their difference in geometry lets the delivery of different amount of healing agent at the cracked site. Definitely, macrocapsules methodology represents the ideal solution to use both for the quantity of preserved healing agent and for the adequate protection that they offer before its release. Nowadays, norms or guidelines that regulate their use do not exist so solutions to be used must be sought in relation to various factors such as capsule/sealant/matrix compatibility, environmental conditions, expected extent of damage and so on.

In this work, the efficiency of self-healing of cement-based materials was investigated. Mortar specimens were produced by incorporating macro-capsules containing precursors of polyurethane; each healing systems was characterized in terms of composition and coating of the shell, position and dimension of capsules. In order to evaluate the self-healing efficacy, the specimens were pre-cracked through a flexural test and, after the time necessary to allow the chemical stabilization of the sealant, the recovery in terms of durability and mechanical properties was verified, respectively, through water flow test and mechanical reloading. The results were subsequently correlated with the spreading areas of the healing agent over the crack faces, in order to check how the mechanism of healing agent released from the capsules may affect the overall system performance. The individuation and quantification of the covered regions was performed through the segmentation of the images of the fracture surfaces. In detail, after correcting the optical defects of the acquired pictures, images have been automatically classified into their components thanks to a pixel-based search, namely the testing plugin learned from images that the user selected for each constituent to then perform the same

analysis on the rest of unknown data, combining machine learning algorithms. Comparing the results, it was established that there is not a strong correlation between the percentage of covered area and the recovery of permeability and mechanical characteristics. On the contrary, it was observed that the evaluation of the spatial distribution of the healing agent is more indicative. In fact, the occupied part of the crack surface influences the tortuosity of the water path and the stiffness contribution of the sealant, expressed in terms of moment of inertia. For all the series of specimens, encouraging results were achieved regarding the offered protection against the introduction of aggressive agents from the exterior. In this way, the use of self-healing materials represents an innovative method to increase the service life of the structures, reducing also their environmental impact. Therefore, a more detailed investigation of the properties of these systems must be pursued thanks to future examinations and the definition of Codes to regulate their use has to be promoted.

Contents

I.	Abstract.....	i
II.	Introduction.....	1
1.	Use and maintenance of concrete.....	3
1.1.	Self-Healing in cementitious materials.....	4
1.1.1.	Stimulated Autogenous Self-Healing.....	4
1.1.1.1.	Nonencapsulated stimulated autogenous healing methods.....	6
1.1.2.	Encapsulated autonomous healing methods.....	7
1.1.3.	Other autonomous healing methods.....	9
1.2.	External treatments.....	11
1.3.	Reporting of cases actually investigated.....	12
1.3.1.	Experimental details for A_CAP.....	12
1.3.1.1.	Materials and compositions.....	12
1.3.1.2.	Specimens casting.....	17
1.3.2.	Experimental details for B_CAP.....	19
1.3.2.1.	Materials and compositions.....	19
1.3.2.2.	Specimens casting.....	20
1.3.3.	Experimental details for RRT5.....	21
1.3.3.1.	Materials and compositions.....	21
1.3.3.2.	Specimens casting.....	22
1.3.4.	Experimental details for CCAP_S.....	23
1.3.4.1.	Materials and compositions.....	23
1.3.4.2.	Specimens casting.....	24
1.3.5.	Experimental details for CCAP_L.....	25
1.3.5.1.	Materials and compositions.....	25
1.3.5.2.	Specimens casting.....	26
2.	Experimental characterization of self-healing systems.....	27
2.1.	Techniques for pre-cracking.....	27
2.2.	Methods for characterization of self-healing efficiency.....	28
2.3.	Tests and results of cases actually investigated.....	31
2.3.1.	Experimental details for Pre-cracking methods.....	31
2.3.1.1.	Setup, results and outcomes for A_CAP.....	34
2.3.1.2.	Setup, results and outcomes for B_CAP.....	36

2.3.1.3.	Setup, results and outcomes for RRT5.....	38
2.3.1.4.	Setup, results and outcomes for CCAP_S.....	38
2.3.1.5.	Setup, results and outcomes for CCAP_L.....	39
2.3.2.	Experimental details for Water Flow test.....	40
2.3.2.1.	Results and outcomes for A_CAP.....	44
2.3.2.2.	Results and outcomes for B_CAP.....	45
2.3.2.3.	Results and outcomes for RRT5.....	46
2.3.2.4.	Results and outcomes for CCAP_S.....	47
2.3.2.5.	Results and outcomes for CCAP_L.....	48
2.3.3.	Experimental details for Mechanical Reloading.....	49
2.3.3.1.	Results and outcomes for A_CAP.....	50
2.3.3.2.	Results and outcomes for B_CAP.....	52
2.3.3.3.	Results and outcomes for RRT5.....	54
2.3.3.4.	Results and outcomes for CCAP_S.....	54
2.3.3.5.	Results and outcomes for CCAP_L.....	54
3.	Calculation of the spreading area of the healing agent.....	55
3.1.	Digital corrections on GIMP.....	55
3.2.	Quantification of the area on IMAGEJ.....	60
3.3.	Final results.....	64
3.4.	Considerations and drawbacks.....	71
4.	Relations between tests results and spreading areas.....	74
4.1.	Correlation between Water Flow and surface coverage.....	74
4.2.	Evaluation of the moment of inertia of the spreading areas.....	76
4.3.	Correlation between ILR and surface coverage.....	81
4.4.	Correlation between IRL and moment of inertia.....	82
5.	Conclusions and future perspectives.....	85
6.	References.....	87

Introduction

In the last century a necessary consequence of the wide use of concrete was the development of treatments and technologies to cope with the problem of cracking. In fact, most of the structures and infrastructures were built in concrete because its versatility in design and inexpensiveness; nonetheless it is a material extremely sensitive to crack formation considering its low tensile strength. It is evident that the onset of small cracks (of the order of magnitude of 300 μm) does not cause the collapse of the damaged element but it influences unavoidably its serviceability. In fact, the presence of cracks, for example due to structural loads, shrinkage, thermal effects and so on, allows the entrance of aggressive external agents that cause the carbonation of concrete and increase the process of corrosion of the steel reinforcement. Generally, cracks have been repaired with surface treatments, namely the part concerned with the sealing was the external one leaving the internal area damaged. Nowadays, the methods of intervention have changed. The idea was to create active and sustainable methodologies. This means that they had to be active to treat the fracture from inside and ecologically sustainable to reduce concrete use thus carbon dioxide emissions for its production. All these targets were concretely pursued through the self-healing cement-based materials. They must be introduced inside the matrix during the construction phase, in order to store and preserve the healing agent before the crack occurs. They were developed to improve the physiological self-repairing mechanisms of concrete, concerning physical, chemical and mechanical processes. Self-healing strategies generally include nonencapsulated and encapsulated technologies. The substantial difference between the two lies in the way the healing agent is kept. The former are incorporated inside the matrix in form of admixtures or additions, while the latter consist in micro or macrocapsules that allow the direct internal availability of the sealant at the location of damage. In the current state, guidelines that regulate their use do not exist but thanks to experimentations it is clear that the adoption of macrocapsules is the most effective healing system in terms of amount of stored agent, product conservation, resistance of the capsules, isolation of the whole system from moisture and external environment.

Therefore, starting from the results achieved in other research and the methodologies available in literature, for this work mortar specimens were produced by incorporating macrocapsules containing precursors of polyurethane, in order to investigate the efficiency of these self-healing methods. In detail, the aim of this thesis is to test the mechanical and durability recovery of five series of samples, different in terms of composition and coating of the shell, position and

dimension of capsule, to finally find their correlation with the spreading areas of the healing agent.

Each series of specimens was described in its composition, namely from the constituents to the geometry of the matrix but also from the components to the extrusion and coating of the shells. For each series, also reference specimens were realized in order to have elements of comparison to understand the real efficiency of the investigated self-healing systems.

As first step, the samples were pre-cracked through a three-point bending test in order to allow the formation of the crack in a controlled mode. In fact, the idea was to break the samples in the middle section where the capsules were positioned during the casting phase; in this way, when the crack reached the capsules, these have been broken and they were capable to realise the healing agent. Once that the polyurethane had achieved its chemical stabilization, the specimens were subjected to mechanical tests to verify the repair efficiency. In detail, the recovery of the series was analysed in terms of durability through a water flow test and mechanical properties through the reloading test. Practically, the water flow test was realized according to the SARCOS protocol, while the mechanical reloading was performed with the same flexural test used for the pre-cracking phase; obviously, this destructive test was realized for the reference specimens only for the ones still not completely broken by the initial test. The analysis of their performances was finally characterized by the quantification of the spreading area of the healing agent over the crack faces. The individuation and computation of the regions was performed thanks to a plugin of the image processor IMAGEJ, capable to segment the pictures of the fracture surfaces in their components. Essentially, after the correction of the optical defects of the photos through the image editor GIMP, they were automatically segmented in their parts related to the matrix and the agent leaked from the capsules. Practically, the testing plugin learned from images that the user selected for each constituent to then perform the same analysis on the rest of unknown data, combining machine learning algorithms.

Once that all these procedures have been completed, correlations between spreading regions and mechanical parameters have been established. In reality, the description of those areas was done also in terms of spatial distribution of the healing agent, trying to find an explanation of the durability and mechanical results by the analysis of the occupied part of the crack surface. In fact, the importance of assessing the influence of the invaded sector on the tortuosity of the water path and its stiffness contribution, expressed in terms of moment of inertia, wants to be demonstrated among a generic quantification of the area.

1. Use and maintenance of concrete

Concrete is the most used material in the field of application of Civil Engineering; in fact, this is extremely true looking at the infrastructures and, above all, at the structures that have been built in the last century, for a total amount of 30 billion tons of concrete used per year [1]. A massive use of this material comes from its flexibility in design, high compression strength and, in general, low cost [2], [3]. On the other side, because of its low tensile strength, it is extremely prone to the formation of cracks [2]; obviously this aspect is not negatable and negligible in design. For this reason, concrete is generally combined in its application with steel reinforcement but, in general, to avoid a huge use of rebars, it is designed to allow the formation of cracks during the lifetime of the structure. In fact, the presence of small cracks ($<300\text{ }\mu\text{m}$ in width) does not cause the failure of the structure but unavoidably reduces its serviceability [1]. Cracks, in effect, allow the entrance of external aggressive agents that, in more or less long times, make the fractures wider and cause the total corrosion of the steel and this represents a condition that has an inevitable consequence: the collapse of the structure [2], [5]. Cracks develop for several reasons but usually they are caused by structural loads, plastic and drying shrinkage, thermal effects. Their presence reduces the performance of the structure and its durability [3], [4]. Thus, already in the design phase, a proper maintenance plan for the lifetime must be scheduled and then applied during the service life of the structure to ensure its correct structural capacity [3], [6]. It is evident that these estimated strategies and cares have a double negative effect, respectively, on the private/public administration that has to face up extra costs [9] (studies shows that the average total European costs for maintenance are equal to half of the annual construction budget [5]), on the environment that has to stand further CO_2 emissions for the production and transportation of other concrete [1]. Nevertheless, a correct analysis of the damage is fundamental to apply a proper correction: only in this way the maintenance intervention will be not useless [6]. In connection with this, the European standard EN 1504 proposes a classification of defects and their causes and effects [6].

For all these reasons, in the last decades, the idea of research and develop technological solutions for a sustainable maintenance of concrete and for the use of natural resources has grown [7]. The aim is to make the structures reliable; thus, there will be a consequent rise of their durability and service life, reducing their economic and ecological impact. For all these reasons, in the last decades, particular interest has been reserved to the self-healing systems to be introduced in concrete. They were investigated for the first time in 1969 for polymeric materials. Then, in 1979 and 1984 other studies on thermoplastic and cross-linked systems were

published, while in the 90's Dry was the first that realized the introduction of self-healing properties in concrete. Only in 2001, when White et al. published in *Nature* their researches on polymer-based materials, the self-healing potential reached the top of interest [5].

The attention from the scientific community to the self-healing cement based materials is never like now actual; in fact, the COST Action CA15202 – Self-healing As preventive Repair of COcrete Structures (SARCOS), that assembles European researches that are active in this field, is supported financially by the European Commission because of its interest in develop these technologies and norms for products, test standards and design guidelines [4], [11]. Nowadays the exigency of develop sustainable solutions is clear [5], as also the Fib Model Code 2010 underlines [4]; the evolution of self-healing concrete represents the way to go.

1.1. Self-Healing in cementitious materials

A physiological consequence of the development of the technologies related to concrete, for example thinking about the high-performance concretes and their higher brittleness respect to the normal ones, is the progress of new methodologies for its maintenance and treatments. Usually a treatment methodology can be, conventionally, passive or active. The former indicates that the crack is cured through an external operation, the latter refers to the technologies, already included at the construction stage, that treat the fracture inside [1], [6]. The last ones are well known as self-healing techniques. A short description of the main self-healing techniques and strategies developed so far by the international scientific community is reported below.

1.1.1. Stimulated Autogenous Self-Healing

The autogenous self-healing capacity in cement-based materials is the intrinsic ability to close cracks and restore partially the mechanical properties of the initial composite thanks to physical, mechanical and chemical reactions within the cementitious matrix [4]. The recent development of self-healing materials works to increase and improve this natural ability, trying also to control the overall behaviour. The improvement of autogenous self-healing capacity is necessary because it results efficient only for restore small cracks (usually 10-100 μm , only in special cases 200 μm) [4]; moreover, it is an unpredictable phenomenon because it is extremely addicted from several factors [5].

The most important mechanisms that produce autogenous self-healing are two [4], [5]; they are:

- Continuing hydration of unhydrated cement grains;
- Precipitation of calcium carbonate crystals $CaCO_3$ on the crack faces according to the Equation (1):



i.e. it comes from the reaction of calcium ions Ca^{2+} of concrete matrix and carbonate ions CO_3^{2-} present in water or in carbon dioxide CO_2 from the incoming air.

Autogenous self-healing is also related to other mechanisms [4], [5] such as:

- Swelling of hydrated cement paste due to water absorption by calcium silicate hydrates;
- Mechanical blocking of the crack by debris or fine concrete particles or impurities moved by water.

All these mechanisms are properly illustrated and graphically described in **Figure 1.1**.

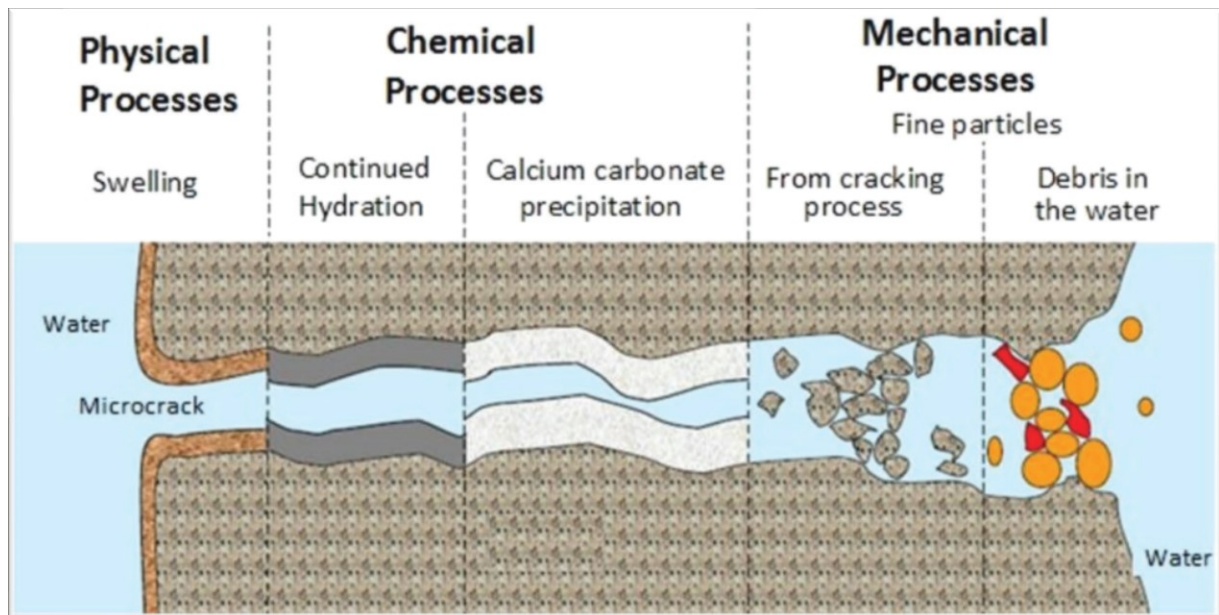


Figure 1.1. Mechanisms involved in autogenous self-healing processes of cementitious materials [4].

As anticipated before, the autogenous self-healing capacity is a non-presumable event because it is influenced by different factors and parameters [3], [4] as:

- Age and composition of the matrix in term of clinker contents, silicate additions, aggregate type, concrete class and age. It is proven that healing in early age concrete is more prolific;

- Water presence that is useful for chemical reactions and the transportation of particles; its presence affects the cementitious environment in terms of temperature, pressure and PH. The most favourable condition consists in water immersion while the worst one in air exposure.
- Geometry and shape of the crack that according to length, depth and width sets if the physiological closure of the crack can happen. Obviously, the narrower are the curable ones. For this reason, usually fibre additions are used to modify the cementitious matrix; in reality, their presence ensures also an additional absorption of water.

Thus, considering all these factors, several technologies able to lead this natural capacity have been developed, creating the so-called stimulated or improved autonomous healing methods. Generally, they are classified in encapsulated and nonencapsulated ones.

1.1.1.1. Nonencapsulated stimulated autogenous healing methods

It is remarkable the use of [4]:

- Mineral additions: they affect hydration kinetics and the material properties. Usually, they are introduced in form of blast-furnace slag and fly ash;
- Crystalline admixtures: the term refers to an admixture dosage which is typically 1% by cement weight for crystalline admixture and >5% for supplementary cementitious materials. They have a considerable hydrophilic behaviour because, reacting with water, form precipitates that enhance the density of concrete and obstruct the penetration of external agents;
- Superabsorbent polymers: from a chemical point of view, they are natural or synthetic 3D crosslinked homopolymers or copolymers with high capacity to absorb fluid. If they are introduced in the matrix, they increase freeze-thaw resistance. In general, they improve the concrete behaviour because they harden after the reaction with the matrix; in fact, they leave macropores that during the fracture phenomenon will be crossed by cracks, allowing the formation of narrow ruptures. Regarding at sustainable solutions, they are introduced in form of proteins or natural backbone grafted with synthetic monomers;
- Non superabsorbent polymers additions: in terms of final product, this category includes the polymer-modified concrete. Their self-ability of healing comes from the interaction of the polymers with the mineral binder. The efficiency of the system depends also on polymer type and dosage, cement type and water/cement ratio. From tests, good results

have been achieved for epoxy resin [4]. Recently other polymers have been investigated, such as shape memory polymers and multiple drawn shape memory polymers. Both are capable to maintain the crack closed, recovering the original shape of the matrix [4].

1.1.2. Encapsulated autonomous healing methods

These solutions allow to locate the healing agent in the damaged location [4], [5]; obviously they must be introduced into the matrix already at the construction phase. The developed technologies are used and tested in form of:

- Microencapsulation: it means that capsules with a diameter smaller than 1 mm are created; it represents a common solution to use [4]. From a practical point of view, the microcapsule is directly embedded in the matrix during the casting of the specimen; when the crack reaches the capsule, it is able to break it and the stored healing agent can fill the fracture occupying its volume. Considering that the healing agent has to remain into the shell for a certain time, the most important aspect to considering when the composition of the capsules has to be designed is the proper conservation that they can provide to the core. For this reason, a double-walled shell usually is employed and generally it is made up of thermally stable and hydrophobic materials. Typical examples of used materials for shells are polyurea and silica-based substances [5]. Also their behaviour has to be properly studied: they must preserve their integrity until the fracture occurs. Thus, the aim is to design a shell that shows an elastic and flexible return in construction phase but when it is finally hydrated it becomes more brittle. During the laboratory tests [2], [7], [8], [10], it has been proved that the fracture mechanism is conditioned by the interaction capsule-matrix; therefor, the chemical compatibility of both parts has to be investigated and improved: only in this way there will be an optimal conformity at the interface. Despite of these attentions to consider when the shell is designed, also the chemical composition of the healing agent has to be investigated. It has to be long term functional and able to react within the matrix; thus, two parts systems are usually adopted. Moreover, the sealing of the crack has the aim to recovery durability and mechanical properties of the cracked element; the improvement is function of capsule fraction, pre-damage level, type of microcapsules used [4]. It has been shown [5], [8] that the mechanical recovery is proportional to the dosage of the microcapsules. It is evident that also how their presence influences the mechanical and durability properties of the matrix has been investigated through experimentation [5], [8];

- Macroencapsulation: the explained considerations in the paragraph above are valid also in this case. It is evident that the geometry of the capsules changes, becoming bigger [2], [4], [5], [7], [8], [10]. For this reason, a higher amount of healing agent can be stored and the sealing efficiency of these type of capsules is superior. The first material investigated for their composition has been the glass but, during the tests, it has been shown [4] that its presence is harmful for the concrete because of the alkali-silica reactions that can happen. Thus, ceramic capsules have been preferred [4]. Recently, the polymeric capsules have been adopted because they allow to work with lower temperatures but also for their easier extrusion [4]. Usually, they are produced in spherical or cylindrical shape. The latter have ordinarily a variable diameter between 0.8 mm and 5 mm; this variation range ensures that the gravitational and capillary forces applied on the healing agent from the exterior are bigger than the ones applied from the inside of the capsule. An alternately solution consists into the substitution of part of the aggregates with others that have been filled with healing agent [4]. Also in this case, to improve the adhesion matrix-capsule, the shell is surrounded with sand [2], [10], [8]; a graphical representation of the methods is provided in **Figure 1.2**.

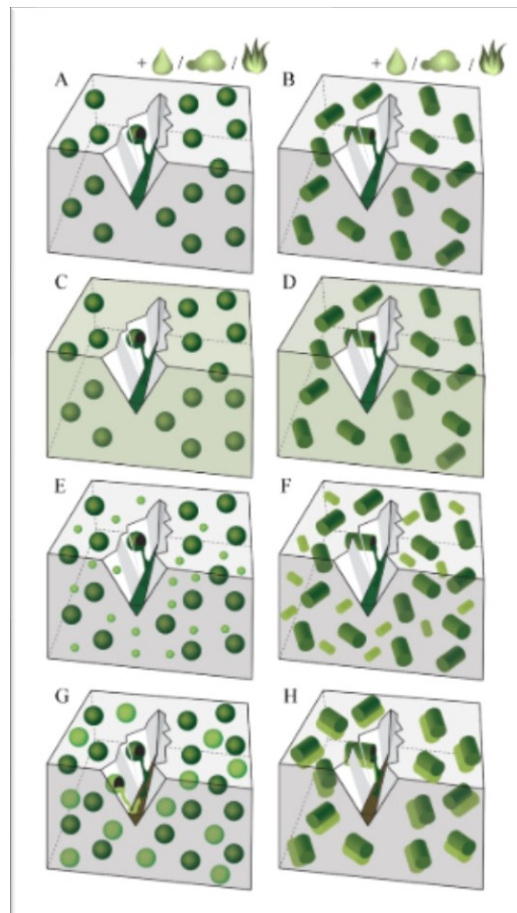


Figure 1.2. Settings of encapsulated healing agents [5].

- Bioconcrete: the production of calcium carbonate can be improved by bacteria thanks to the induced precipitation [1], [9], [17]. This effect is emphasized in wet-dry environment. The bacteriological colony that has been investigated is the ureolytic one; it has been demonstrated [9] that its application is optimal in cementitious materials. Also dormant bacterial spores have been used to produce carbon dioxide that is functional to the precipitation of limestone; this process is also known as metabolic aerobic degradation [4]. Other studies [4] have been led on denitrifying bacteria because they allow the precipitation in low oxygen conditions; in fact, in this case, only the nitrate is necessary to initiate their activity. In general, the precipitation of calcium carbonate requires an optimal environment, adequate pH value and sufficient nutrients for bacteria. The process is described also in **Figure 1.3**. To reduce the risk of losing a culture in the matrix, they are usually added as encapsulated or immobilized within porous carriers. Their encapsulation is simple because they are inert, solid and insoluble in water. A recent discover expects the encapsulation in hydrogel; this technology allows to maintain active spores during the storage and then, after the capsule's break, to be a reserve for germination [4].

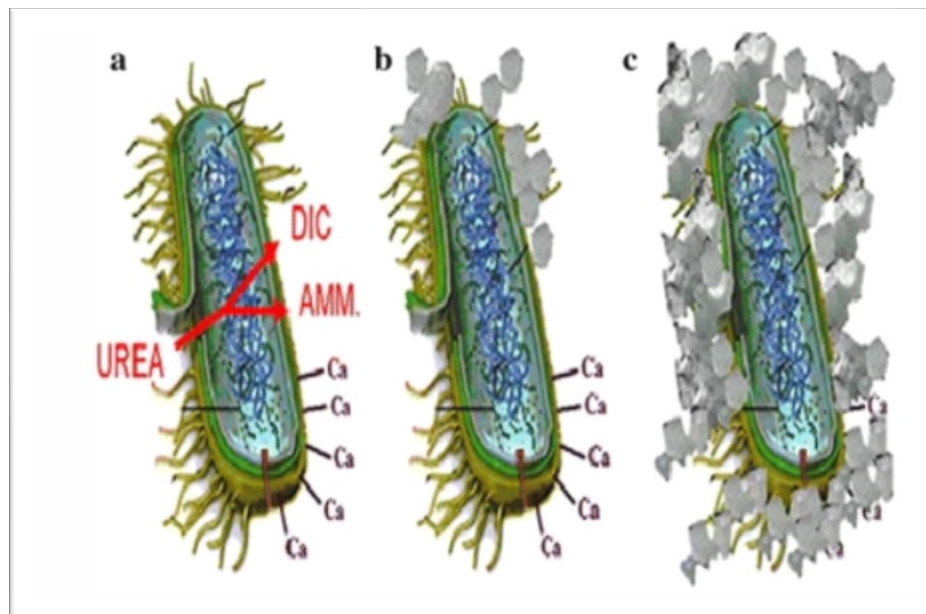


Figure 1.3. Precipitation of calcium silicate involved in the healing process [17].

1.1.3. Other Autonomous healing methods

The last useful method in perspective of sustainable solution consists into the formation of:

- Vascular system: the idea is to create a vascular network that can deliver the healing liquid to the damaged area [5]. If the agent is provided by an external source, the system

can be used infinite times. Moreover, this could allow to inject different types of healing agents, curing the damage in a more proper way. The system works with the healing liquid pumped inside the matrix under pressure. The simplest way to realize the system is with a 1D channel; a more complex version, instead, it is made up of 2D or 3D channels. A graphic representation is reported below in **Figure 1.4**. Practically, a vascular system is created with immersed capillary tubes in concrete that are able to support the matrix casting or through tubular moulds that are removed after the concrete casting in order to leave at their place holes; the development of recent technologies allows also to create a 3D printed version of the vascular channels [4]. In reality, at the state of facts, the application of these systems is restrained by two not fixed problems: the continuous contact with the atmosphere and the unviable human intervention for their use.

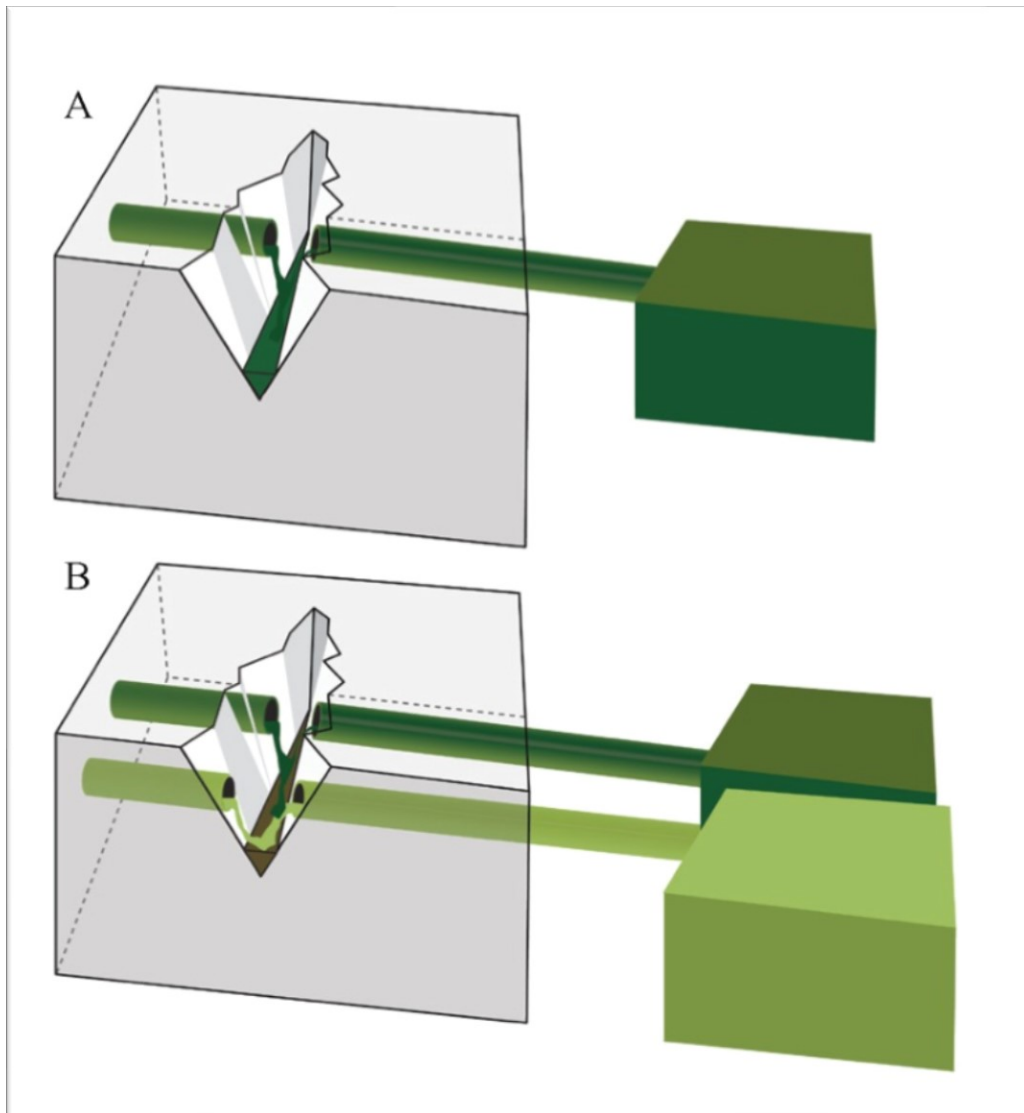


Figure 1.4. Vascular systems devices [5].

1.2. External treatments

The principal aim of these methods is to protect the damaged structure from the entrance of aggressive agents and moisture curing the superficial surface; moreover, they have to treat the decrease of durability and mechanical properties of the cracked elements [4], [6]. This can be done through:

- Repairing materials: the repair zone surface is the weak part of the structure because its chemical, physical and electrochemical differences respect to the rest. Commonly polymer-modified materials, geopolymers, high performance fibre reinforced cementitious composites and textile reinforced concrete are used [6]. The repair is successful if the restored zone is stronger than the substrate: only in this way there will be not again the formation of new cracks in the same area;
- Protection from penetration of air and water: the external surface covers and protects the inner zone from aggressive agents such as moisture and particles that can produce a chemical attack. To avoid these uncomfortable conditions, waterproofing treatments with hydrophobic material or pore blocking surface treatments through sodium silicate are applied [6];
- Injection technique: the introduction of sealing material has the aim to fill cracks and voids. It consists into the injection into the system of cement slurries or polymers through high pressure and the consequent filling of the damaged zones thanks to the action of gravitational forces. Another technique consists in electrodeposition; it allows both the filling of the fracture and the physical protection of the substructure [6];
- Smart functionalities: a new class of healing agents is represented by nanocomposite coatings because they are capable to penetrate the surface that they have to cover [6]. Recent studies on bioformulation and biodeposition of concrete, iron-based bioproducts, polymer-based bioproducts and nanosilica have been conducted [6].

1.3. Reporting of cases actually investigated

As described before, actually there are not known solutions or combinations of materials that can be applied for specific cases [2], [4], [6]. In fact, the idea is to define tailored solution for real operating systems to treat; this implies a proper selection of the healing agent and of the capsules' locations thinking to all the mechanisms of interaction and coexistence between the healing system and the matrix. Another aspect to cure is the dimension of the capsules to introduce, considering the capillary forces that could act and the shells interferences on the mechanical properties of the specimen [4]. As specified before, the environmental conditions of the matrix influence the conservation and the durability of the core; for this reason, also the investigation of the coating layers is fundamental, in order to isolate the agent from the exterior [1], [2], [4], [8], [10]. Thus, considering all these factors, it is appropriate that accurate laboratory investigations are led but, above all, that tests are carried out under real environmental conditions. This paragraph contains a reporting about the cases actually studied and the investigations conducted; part of the specimens has been realized during a laboratory exercitation while the remaining part comes from studies group led for international experimentations.

1.3.1. Experimental details for A_CAP

These specimens have been casted for the exercitation of the Course in *Testing of materials, models and structures*. It is presented below a description of components, realization techniques and relative required times.

1.3.1.1. Materials and compositions

The investigated healing system has been carefully defined in terms of:

- Shell:

As first step, all the ingredients have been weighed and then mixed together but separating the solid components from the liquid ones; only at the end, all these are mixed together through an overhead stirrer. The shell is made up of:

- A solid part of:
 - Portland cement CEM I 52,5 R (217 g);

- Calcium Carbonate CaCO_3 (100 g): it has the purpose to increase the stiffness of the cementitious matrix during the extrusion phase;
 - Metakaolin (1,6 g): it is added to reduce the water/cement ratio; the produced geopolymers enhance the compactness of the matrix;
 - Hydroxypropyl methylcellulose HPMC (3,4 g): it is added as a water-retaining agent and as a modifier of the viscosity to reduce segregation of components and to improve homogeneity and workability;
- A liquid part of:
- Demineralized water (60 g);
 - PRIMAL B 60 A (80 g): it is a copolymer of methyl methacrylate and ethyl acrylate used as densifying;
 - Poly(ethylene glycol) PEG (8 g): it reduces the shrinkage of concrete with a minimal effect on strength.

The mix was finally worked by hands to allow the evaporation of the water in excess. The shells have been realized on a neoprene surface, trying to form tubular capsules around a thin cane with a diameter of 6 mm. After the modelling phase, the capsules were stored inside a controlled environment for 3 days. After the extraction from the formwork, their geometry has been controlled and adjusted, trying to obtain all the macrocapsules with a length of 5 cm. At the end, they were kept in air at room conditions for 4 days. Photos of these steps and of the final result are attached below in **Figure 1.5**.



Figure 1.5. Shell extrusion and final products.

- Coating and block of extremities:

In order to avoid the absorption of water and moisture by both the internal and external walls of the shell, respectively from the stored healing agent and the matrix, the capsules have been coated with a PRIMER AQ (Api Spa) by immersion. This is a bi-component epoxy resin and generally it is used only to create a first protective film for the shell. After this step, the capsules were stored vertically in suspension through clips, to remove the excess of applied material, as shown in **Figure 1.6**. The next day, a first layer of coating of PLASTIGEL (Api Spa) was applied with syringe to ensure a complete filling of the cavity without bubbles. The applied resin is highly viscous so they were stored again in suspension to facilitate the drop of the parts in excess; in fact, in this phase, the creation of an homogenous and thin internal coating is fundamental. The next day, one end of the tube was sealed with a two component epoxy-based thixotropic plaster STUCCO K (Api Spa); after 4 days, the healing agent was introduced inside and immediately blocked also on the other side; this procedure has to be made quickly because the agent used as sealer is highly reactive. A second layer of external coating, always using PLASTIGEL, was applied to guarantee a complete protection to the entire system from the exterior. As last step for the coating of the shells, they were rolled in sand; this phase has the aim to improve the adhesion between the two systems. Photos of these steps and of the final result are attached below in **Figure 1.7**.

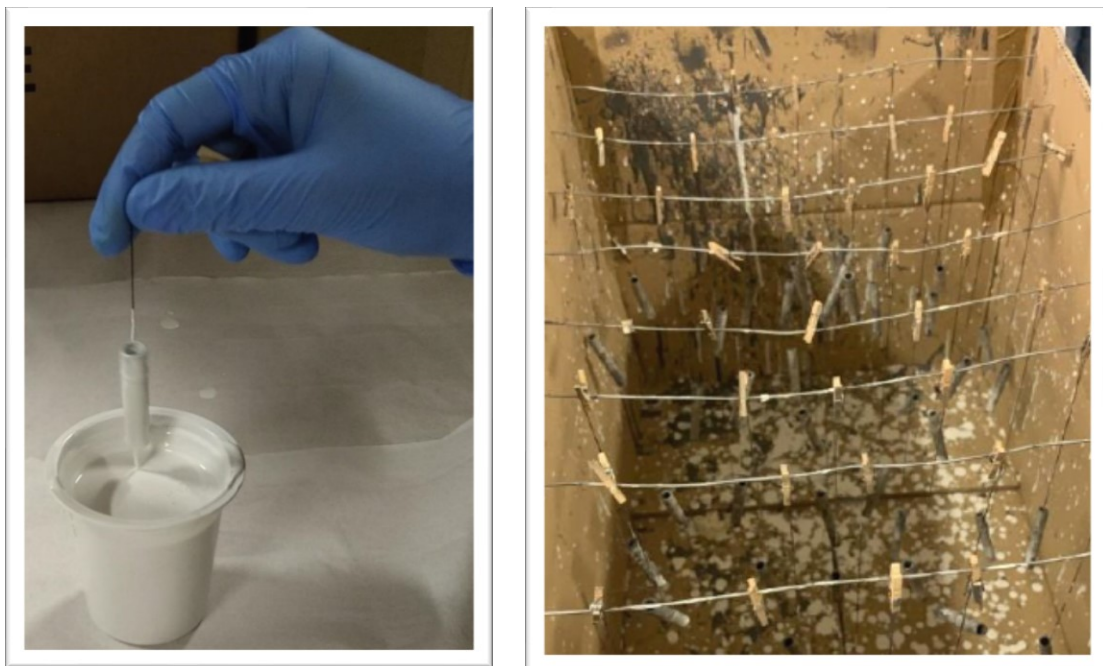


Figure 1.6. Application and suspension of capsules in order to remove the product excesses.



Figure 1.7. Final coating and rolling into the sand of the capsules to improve their adhesion.

- Healing agent:

Regarding to the selected healing agent, for these specimens, the polyurethane precursor CARBOSTOP U (Orica Spa) was used. It consists of modified polyisocyanates with additives; reacting with ambient water it creates a polyurethane/polyurea foam. It is assumed that the product temperature is between 15°-30°C before processing and during application. At this condition, the viscosity goes from 270 to 2500 mPa*s, while the foam factor (free rise) varies between 30-60 [23]. The final aspect of the filled capsules is reported below in **Figure 1.8**.

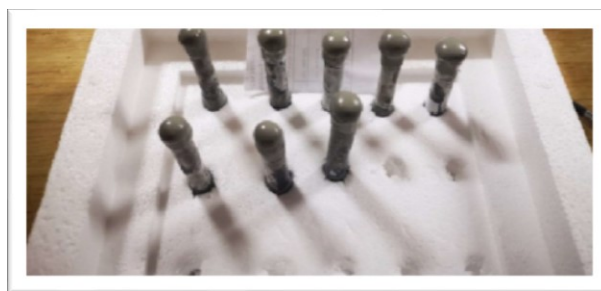


Figure 1.8. Filling of the capsules with the healing agent and blocking of their extremities.

- Matrix:

The efficiency of the capsules was investigated in mortar specimens. The mortar was created with a water-to-cement ratio of 0.5 and a sand-to-cement ratio of 3 and an

ordinary Portland cement CEM I 42,5 R, according to the following quantities:

- CEM I 42,5 R (450 g);
- Water (g);
- Sand (1350 g)

The mixing procedure was made according to the prescriptions of the Standard UNI EN 196-1 [12]; the mixing procedure (illustrated in **Figure 1.9.**) shall be as follows:

- place the water and the cement into the bowl, taking care to avoid loss of water or cement;
- immediately after the water and cement are brought into contact, start the mixer at the low speed while starting the timing of the mixing stages. In addition, record the time to the nearest minute, as ‘zero time’. After 30 s of mixing, add the sand steadily during the next 30 s. Switch the mixer to the high speed and continue the mixing for an additional 30 s. Note: ‘Zero time’ is the point from which the times for demoulding specimens and for determining strength are calculated.
- stop the mixer for 90 s. During the first 30 s, remove by means of a rubber or plastics scraper the mortar adhering to the wall and bottom part of the bowl and place it in the middle of the bowl;
- continue the mixing at the high speed for 60 s.



Figure 1.9. Preparation of mortar mixture.

1.3.1.2. Specimens casting

The fresh conglomerate was used to fill prismatic moulds of dimensions 40 by 40 by 160 mm³ as it is possible to see in **Figure 1.10**. For tests, two series of samples were created:

- first set made up of 6 specimens containing 2 capsules and the hole for the water flow test;
- second set made up of 6 specimens containing only the hole for the water flow test; in sake of simplicity, they are called in the report with the name A_REF. These specimens are used to compare the two sets and to investigate the real efficiency of the applied healing system.



Figure 1.10. Casting of specimens in prismatic moulds and positioning of capsules inside.

To realize all this, as first step, the moulds have been covered with a demoulding oil; then the capsules and the smooth steel bar (with a diameter of 5 mm and covered itself with the

demoulding oil) were placed in position in the mould thanks to the help of nylon threads to fix their position. In detail, the capsules were placed at 10 mm from the bottom side of the specimens while the bar was positioned centrally, with its centre at 15 mm from the top side of the specimen, as schematically reported in **Figure 1.11**. Subsequently, the specimens were casted and then stored in an air-conditioned room. The day after casting, the steel bar was removed from the specimens; while the specimens were demoulded after 2 days from the casting and subsequently stored for other of 10 days in controlled air conditions.

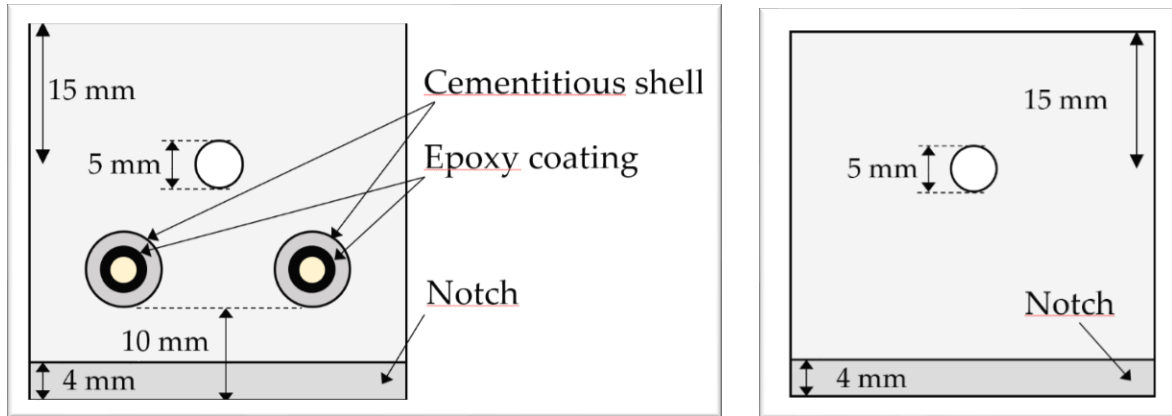


Figure 1.11. Geometrical positions of capsules and hole for A_CAP and its REF.

1.3.2. Experimental details for B_CAP

These specimens have been casted for the exercitation of the Course in *Testing of materials, models and structures*. Realization techniques and relative required times are identical to the A_CAP ones; thus, for these details, it is recommended to refer to the *Paragraph 1.2.1*. Instead, the components are listed below.

1.3.2.1. Materials and compositions

The investigated healing system has been carefully defined in terms of:

- Shell:

It is made up of:

— A solid part of:

- Portland cement CEM I 52,5 R (217 g);
- Calcium Carbonate CaCO_3 (100 g);
- Metakaolin (1,6 g);
- Hydroxypropyl methylcellulose HPMC (3,4 g);

— A liquid part of:

- Demineralized water (60 g);
- PRIMAL B 60 A (80 g);
- Poly(ethylene glycol) PEG (8 g).

- Coating and block of extremities:

In order to isolate the capsules, they have been coated and sealed with:

— Internal layers:

- Primer AQ;
- Plastigel;

— Extremes blocking:

- Stucco K;

— External layers:

- Plastigel;

- Sand.
- Healing agent:

The polyurethane precursor CARBOSTOP U (Orica Spa) was used.

- Matrix:

The efficiency of the capsules was investigated in mortar specimens. The mortar was created with a water-to-cement ratio of 0.5 and a sand-to-cement ratio of 3 and an ordinary Portland cement CEM I 42,5 R, according to the following quantities:

- CEM I 42,5 R (450 g);
- Water (250 g);
- Sand (1350 g).

1.3.2.2. Specimens casting

The fresh conglomerate was used to fill prismatic moulds of dimensions 40 by 40 by 160 mm³. For tests, two series of samples were created:

- first set made up of 6 specimens containing 2 capsules;
- second set made up of 6 specimens; in sake of simplicity, they are called in the report with the name B_REF. These specimens are used to compare the two sets and to investigate the real efficiency of the applied healing system.

The capsules were placed at 10 mm from the bottom side of the specimens as schematically reported in **Figure 1.12**.

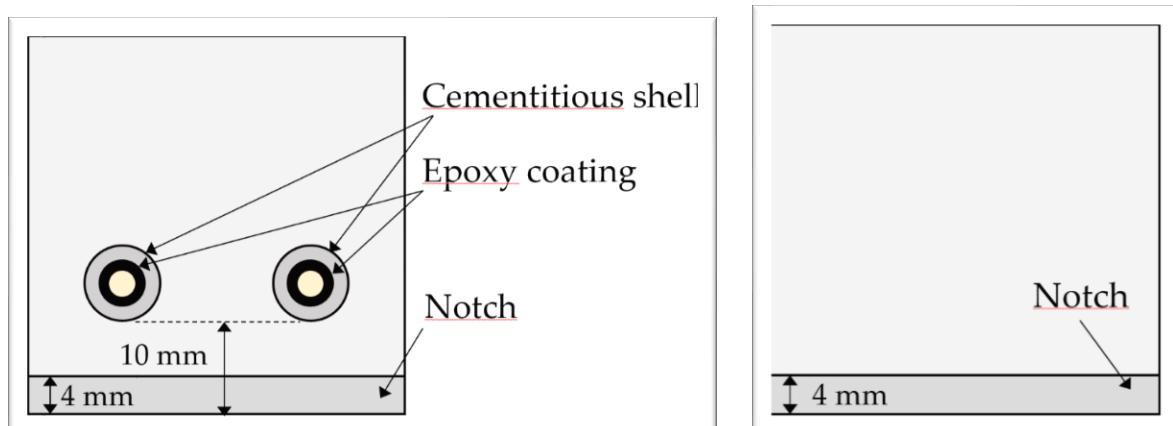


Figure 1.12. Geometrical positions of capsules for B_CAP and its REF.

1.3.3. Experimental details for RRT5

These specimens have been casted for an inter-laboratory study for a European research project. Realization techniques, relative required times and components are listed below.

1.3.3.1. Materials and compositions

The investigated healing system has been carefully defined in terms of:

- Shell:

The macro-capsules were made from borosilicate glass with an external and internal diameter, respectively, of 3,35 mm and 3 mm.

- Block of extremities:

In order to block the extremes of the capsules a two-component epoxy glue was used (PC 5800, Tradecc). In this case, no external or internal coating was applied to increase the isolation of the core.

- Healing agent:

Regarding to the selected healing agent, for these specimens, a single-component liquid polyurethane (HA Flex SLV AF) was used. It has a low viscosity and it polymerizes when it comes in contact with moisture. It shows a viscosity of 200 mPa*s at 25 °C [24]. The polyurethane has a natural weak yellow colour but to make it more visible once distributed over the specimen a small amount of bright yellow fluorescent powder dye (EpoDye, Struers) was mixed into the polyurethane, before the filling step.

- Matrix:

The efficiency of the capsules was investigated in mortar specimens. The mortar was created with a water-to-cement ratio of 0,5 and an ordinary Portland cement CEM I 42,5 N, according to the following quantities:

- CEM I 42,5 N (519 kg/m³);
- Water (257,7 kg/m³);
- Sand (0-2 mm) (1313,1 kg/m³);

- Limestone filler (89,0 kg/m³);
- Superplasticizier Master Glenium 27 (787 ml/m³)

The mixing procedure was made according to the prescriptions of the Standard UNI EN 196-1 [12].

1.3.3.2. Specimens casting

The fresh conglomerate was used to fill prismatic moulds of dimensions 40 by 40 by 160 mm³. For tests, two series of samples were created:

- first set made up of 6 specimens containing 2 capsules and the hole for the water flow test;
- second set made up of 6 specimens with only the hole for the water flow test; in sake of simplicity, they are called in the report with the name RRT5_REF. These specimens are used to compare the two sets and to investigate the real efficiency of the applied healing system.

The capsules were placed at 5 mm from the bottom side of the specimens while the bar to create the hole for the flow test, with a diameter of 5 mm, was positioned centrally, with its centre at 15 mm from the bottom side of the specimen as schematically reported in **Figure 1.13**.

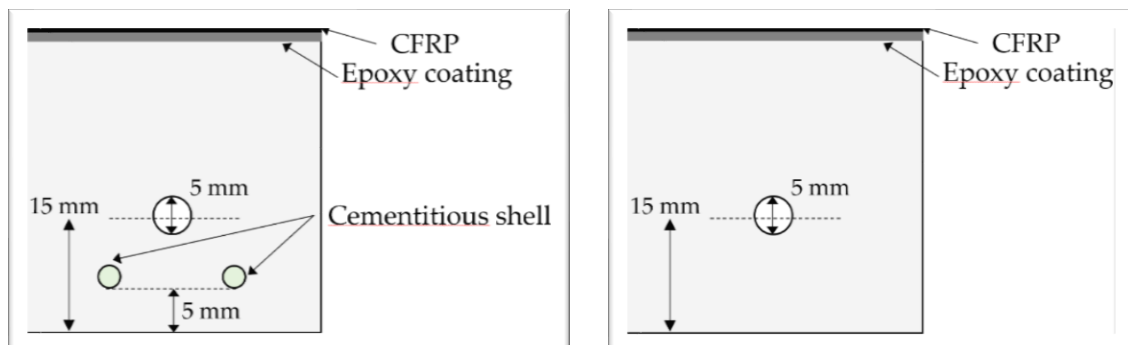


Figure 1.13. Geometrical positions of capsules and hole for RRT5 and its REF.

A Carbon Fibre Reinforced Polymer (CFRP) strip, embedded in epoxy resin, with dimensions of 40 mm by 160 mm, was glued on the top side of the specimens in order to cause the creation of a narrower crack after the tests because it does not allow that the two halves have a relative rotation around their axis [1].

1.3.4. Experimental details for CCAP_S

These specimens have been casted for a project presented at the 7th International Conference on Self-Healing Materials (ICSHM2019). Realization techniques, relative required times and components are listed below.

1.3.4.1. Materials and compositions

The investigated healing system has been carefully defined in terms of:

- Shell:

The macro-capsules were made of cementitious components with an external and internal diameter, respectively, of 5 mm and 8 mm for a total longitudinal length of 60 mm. They were produced by rolling.

- Block of extremities:

In order to isolate the capsules, they have been coated and sealed with:

- Internal layers:

- Epoxy primer (Primer AQ) applied by immersion;
- Epoxy resin (Plastigel) applied by injection;

- Extremes blocking:

- Epoxy plaster (Stucco K);

- Healing agent:

Regarding to the selected healing agent, for these specimens, a liquid single-component polyurethane (HA Flex SLV AF) was used. It has a low viscosity and it polymerizes when comes in contact with moisture. The PU has a natural weak yellow colour but to make it more visible once distributed over the specimen a small amount of bright yellow fluorescent powder dye (EpoDye, Struers) was mixed into the PU, before the filling step.

- Matrix:

The efficiency of the capsules was investigated in mortar specimens. The mortar was created with a water-to-cement ratio of 0,5 and a water-to-sand ratio of 3 and an ordinary Portland

cement CEM I 42,5 N. The mixing procedure has been made according to the prescriptions of the Standard UNI EN 196-1 [12].

1.3.4.2. Specimens casting

The fresh conglomerate was used to fill prismatic moulds of dimensions 40 by 40 by 160 mm³. For tests, two series of samples were created:

- first set made up of 6 specimens containing 2 capsules and the hole for the water flow test;
- second set made up of 5 specimens with only the hole for the water flow test; in sake of simplicity, they are called in the report with the name CREF_S. These specimens are used to compare the two sets and to investigate the real efficiency of the applied healing system.

The capsules were placed at 3 mm from the bottom side of the specimens while the bar to create the hole for the flow test, with a diameter of 5 mm, was positioned centrally, with its centre at 15 mm from the bottom side of the specimen as schematically reported in **Figure 1.14**.

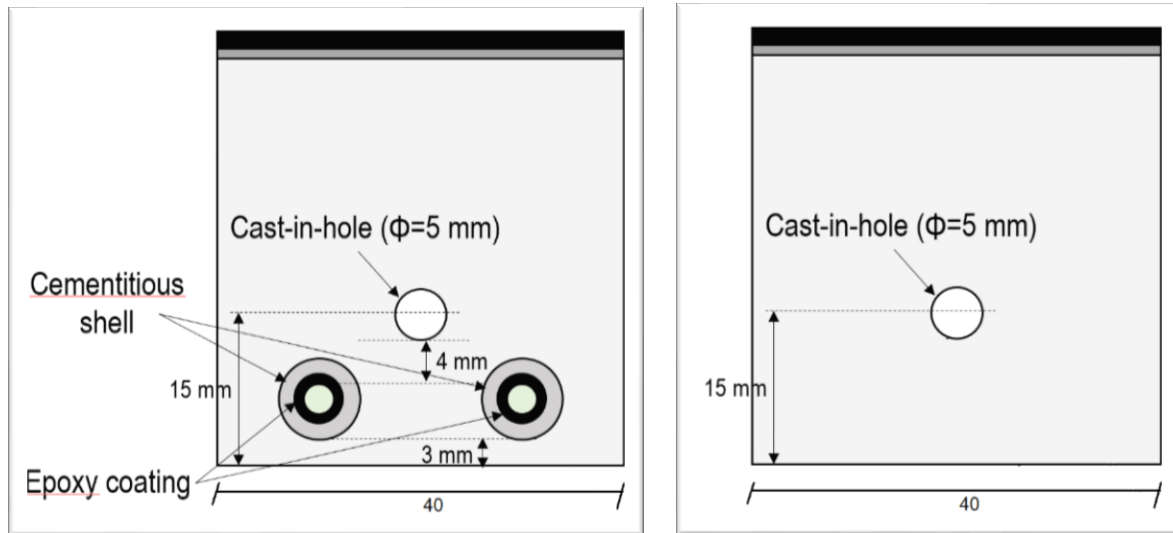


Figure 1.14. Geometrical positions of capsules and hole for CCAP_S and its REF.

A Carbon Fibre Reinforced Polymer (CFRP) strip, embedded in epoxy resin, with dimensions of 40 mm by 160 mm, was glued on the top side of the specimens in order to allow a cracking control procedure [1].

1.3.5. Experimental details for CCAP_L

These specimens have been casted for a project presented at the 7th International Conference on Self-Healing Materials (ICSHM2019). Realization techniques, relative required times and components are listed below.

1.3.5.1. Materials and compositions

The investigated healing system has been carefully defined in terms of:

- Shell:

The macro-capsules were made of cementitious components with an external and internal diameter, respectively, of 7,5 mm and 10 mm for a total longitudinal length of 45 mm. They were produced by extrusion.

- Block of extremities:

In order to isolate the capsules, they have been coated and sealed with:

— Internal layers:

- Epoxy primer (Primer AQ) applied by immersion;
- Epoxy resin (Plastigel) applied by injection;

— Extremes blocking:

- Epoxy plaster (Stucco K);

- Healing agent:

Regarding to the selected healing agent, for these specimens, a liquid single-component polyurethane (HA Flex SLV AF) was used. It has a low viscosity and it polymerizes when comes in contact with moisture. The PU has a natural weak yellow colour but to make it more visible once distributed over the specimen a small amount of bright yellow fluorescent powder dye (EpoDye, Struers) was mixed into the PU, before the filling step.

- Matrix:

The efficiency of the capsules was investigated in mortar specimens. The mortar was created with a water-to-cement ratio of 0,5, a water-to-sand ratio of 3 and an ordinary Portland cement

CEM I 42,5 N. The mixing procedure has been made according to the prescriptions of the Standard UNI EN 196-1 [12].

1.3.5.2. Specimens casting

The fresh conglomerate was used to fill prismatic moulds of dimensions 40 by 40 by 160 mm³. For tests, two series of samples were created:

- first set made up of 6 specimens containing 1 capsule and the hole for the water flow test;
- second set made up of 6 specimens with only the hole for the water flow test; in sake of simplicity, they are called in the report with the name CREF_L. These specimens are used to compare the two sets and to investigate the real efficiency of the applied healing system.

The capsules were placed at 5 mm from the bottom side of the specimens while the bar to create the hole for the flow test, with a diameter of 5 mm, was positioned centrally, with its centre at 20 mm from the bottom side of the specimen as schematically reported in **Figure 1.15**.

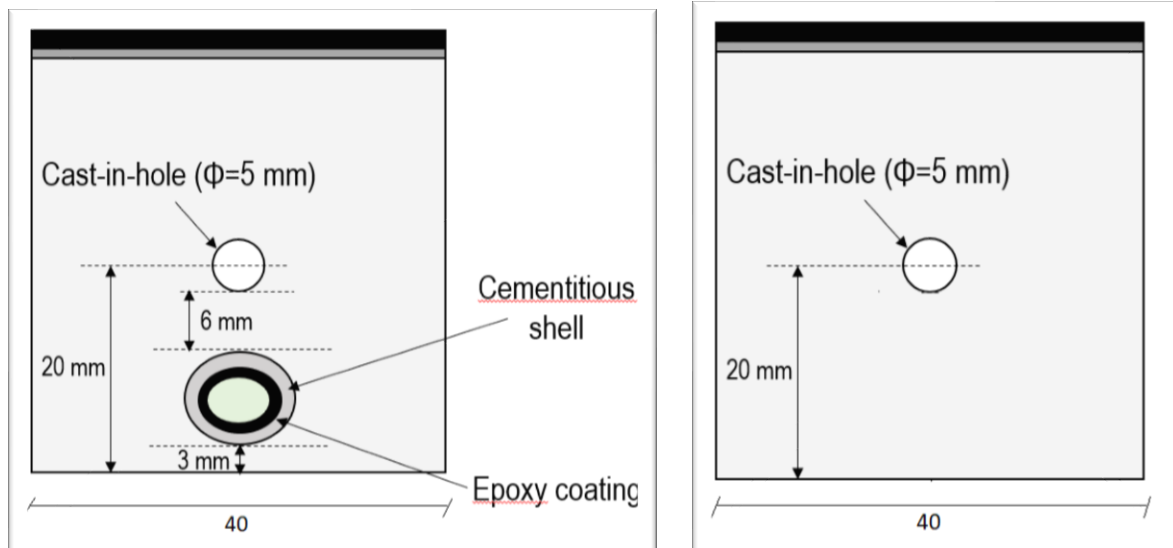


Figure 1.15. Geometrical positions of capsule and hole for CCAP_L and its REF.

A Carbon Fibre Reinforced Polymer (CFRP) strip, embedded in epoxy resin, with dimensions of 40 mm by 160 mm, was glued on the top side of the specimens in order to allow a cracking control procedure [1].

2. Experimental characterization of self-healing systems

The development of self-healing techniques includes also the definition of tests to verify if the mechanism in healing is correct. For this reason, it is necessary that a unified system for the validation and comparative evaluation of these methods is made [3]; it is the aim, for example, of the European research COST [3], [11]. Tests must be capable to verify the recovery of material properties as a direct consequence of the crack sealing. In fact, the filling of a fracture depends not only from the characteristics of the healing agent and its final product but also from external variables, as age and width of crack, environmental conditions, applied load and more from intrinsic features of the matrix, as presence of water and moisture, stress state [3]. Therefore, the correlation between crack closure and restored physical or mechanical properties must be proved through tests because, as described, a lot of variables can affect the final result. It is now reported a list of methods used to quantify the healing efficiency of systems, starting from pre-cracking techniques until mechanic tests.

2.1. Techniques for pre-cracking

Pre-cracking consists into the introduction of a preliminary level of damage into specimen through a controlled way [3]. Thus, localized cracks are performed with technical equipment. During all these tests, it is fundamental that specimens without self-healing technologies are tested in order to evaluate the effectiveness of the healing system; reference specimens must be in the same curing state of the sheltered ones because, as already explained, no factors have to affect the final result. Also the choice of the test to use has to be thoughtfully considered. In fact, a proper selection holds in consideration the used self-healing system, specimens shape, crack shape, type and material of the matrix, characteristics to investigate and real structural situation of action [3]. Tests generally used for pre-cracking are:

- Three or four- point bending tests on notched or unnotched specimens: these tests are generally used, respectively, for studies on beam elements because the first allows the formation of cracks with varying widths, while the second the cracking of plain concrete or ordinary fibre reinforced concrete specimens [3]. Usually, they are performed in closed loop deformation (crack opening) control with notch or in load control with unnotched samples;
- Tensile tests: in general, its application is followed by the evaluation of the resistance to chloride penetration [3];

- Compression tests: this technique is useful to test the recovery of compression strength and its performance after a severe loading action.
- Non-through going cut.

Regardless of the used tests, during their application the evaluation of both the effects of elastic regain on opening upon load removal and the residual crack width after unloading is important [3]. It is evident that the accuracy of the evaluation is highly floating but this is not the only reason that questions the choice of the crack width as a check parameter. In fact, it is an evident and immediate variable to estimate but, considering all the complex mechanisms involved, is uncomplete because it does not permit, for example, the expression of information about the internal conditions. For this reason, X-ray studies are realized [3].

2.2. Methods for characterization of self-healing efficiency

The effectiveness of the self-healing systems is made in terms of evaluation of [3]:

— Crack closure:

As said in the previous paragraph, a parameter that is always chosen to quantify the recovery of a fracture is the crack width; its determination can be performed in two ways, respectively, with naked eye or microscopy techniques. Generally, the most used ones request the use of:

- Photography cameras: periodical pictures are registered to follow the trigger and propagation of cracks and the performance of the sealing agent;
- Light microscopy (optical, digital and stereo): it consists into the investigation of the specimen through radius sources. It is a common analysis to perform;
- Electron microscopy.

Researches [1], [2], [8] agree on the importance to investigate the internal conditions of cracks instead of a limited evaluation of the only superficial state of art. Thus, recently several techniques [3] based on the use of penetrating waves have been developed to examine inside the matrix in form of:

- Fibre optic sensing: it allows a continual spatial and temporal registration of cracks width;

- X-ray radiography or tomography: X-rays that strike the specimen are partially absorbed by constituent objects according to their density and composition; it is evident that a definition of the sample in terms of aggregates/matrix/voids can be done;
 - Neutron radiography or tomography: neutron rays interact with atomic nuclei, showing patterns for X-rays;
 - Computerized tomography scan: it is a technique based on a combination of X-ray waves;
 - Electronical methods: as the definition suggest, they include all the techniques that permit a measure of the electronical properties of the investigated specimen.
- Recovery of engineering effects:
- It is estimated concerning durability; it can be expressed in form of:
- Permeability: it quantifies the amount of diffused liquids or gases; it is estimated through:
 - Decrease in pressure (water height) after a certain period: the specimen is subjected to water penetration; the test consists into the registration of the height changes in the pipette of the water that crosses the sample. Thus, a water permeability coefficient can be defined;
 - Water flow test: it subsists in the evaluation of water that passes through the specimen during a certain period. Recently, in the European project Healcon [3] a standardization of the water flow test was defined. Specimens with a casting in hole must be produced; water is putted in circulation from a basis and its flowing is captured on a scale. Executing the test on a sealed and unsealed specimen, two indices that provide a quantification of the reached level of permeability can be calculated;
 - Sorpitivity: by definition, it is an indicator of concrete ability to absorb and transmit liquids by capillary suction [3]. Experimentally, specimens are cured in an oven to remove moisture. Subsequently, they are partially immersed in water and weighted in prescribed time intervals to determine the acquired mass, until their weight remains constant. Also in this case, permeability is described through an index;
 - Chloride penetration: it is proven that [3] the tortuosity of a crack reduces the ions diffusion through it. For this reason, it is evident that this test

gives an idea of the protection provided to steel reinforcement and of the multiconnection of internal voids. The examination subsists in the evaluation of colour change boundary test and the determination of a chloride diffusion parameter.

- Mechanical properties: all these tests expect a comparison with undamaged and unsealed samples to determine the real action and contribution of the investigated healing system on the achieved recovery. Performed test, obviously, are executed to quantify the mechanical characteristics and to recalibrate, eventually, the healing system. The experimental investigation consists in:
 - Compression test: it provides the application of compressive strength of a quantity equal to a fraction of pre-and-post peak regime;
 - Tensile test: it assesses the recovery of post cracking residual load;
 - Flexural test: generally, three or four-point bending test is executed to quantify the improvement of strength and stiffness. Laboratory experiments prove that the recovery remains slower than the crack sealing.

By this general revision of methods, it is evident that the estimation of the crack closure is the most immediate and physiological way to evaluate the effectiveness of a healing system and, for sure, it consists in non-destructive technique if compared with the mechanical detections. But it is also clear that a microscopic investigation of the healing product is required to verify if its physical and chemical microstructure is appropriate for sealing, despite of its apparently perfect macrostructure as it appears, for example, in the sample shown in **Figure 2.1**.

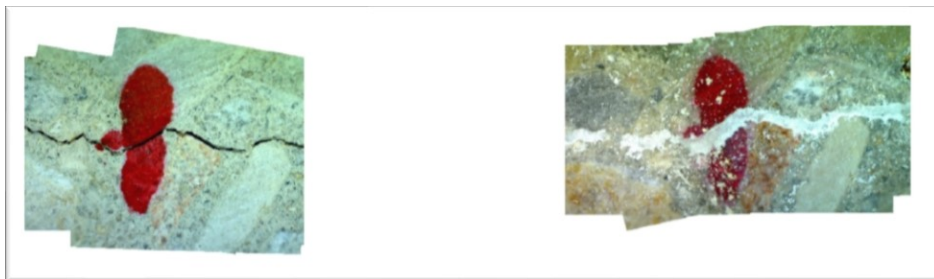


Figure 2.1. Crack sealing and optic evaluation of its width [3].

Usually, just considering the complexity of the healing mechanism, results of tests are returned in terms of correlations between achieved crack closure and recovered mechanical properties.

2.3. Tests and results of cases actually investigated

As described in the previous paragraph, the choice of the test to perform must be carefully thought out according to several factors. For all the series of specimens analysed in this thesis a three-point bending test was chosen for pre-cracking step because it has been considered the most appropriate, thinking also the real conditions to which they will be subjected in service life. Another aspect to underline in this introduction to the reporting is that the pre-cracking stage represents the most important phase for the achievement of a functional spreading of the healing agent. Thus, the three-point bending test seemed the best to perform even according other researches [1], [4], [7], [8], [9], [10]. Moreover, different tests to quantify the reached durability were performed. For each method a general description and the results achieved in laboratory for each series is reported. Please note that not all tests have been performed for each group of samples.

2.3.1. Experimental details for Pre-cracking methods

The three-point bending test allows to create localized damage thanks to its configuration settings in terms of application of loads and placement of the specimen. Its aim is to verify the mechanical behaviour of a damaged specimen after the leakage of the healing agent up to the external surfaces of the specimens. Obviously, the analysis is completed with the comparison of the results of the specimens without an embedded self-healing system. A practical example of the conducted investigations is provided in **Figure 2.2**.

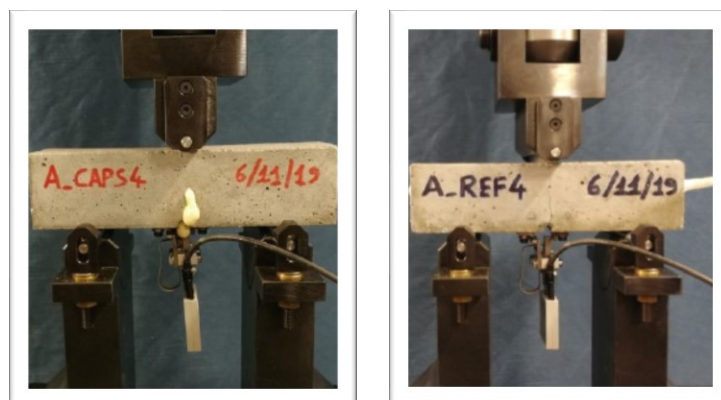


Figure 2.2. Results of pre-cracking test for, respectively, self-healing specimens and reference ones.

There are two ways to perform this test, that is:

- In crack opening control:

In order to realize the test in this mode, a notch is created on the specimen; generally, it is realized already at the casting phase or by a saw-cutting, in a U-shape with a dimension not bigger than 1/10 of its sizes, for example as done in **Figure 2.3**.



Figure 2.3. Notched specimen for the pre-cracking test.

This experimental setting is well-known as crack mouth opening displacement (CMOD) control mode. A photographic report of the devices is available in **Figure 2.4**.

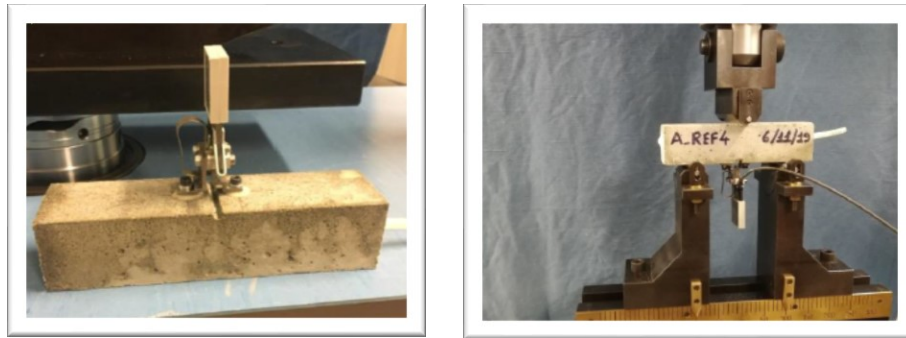


Figure 2.4. Clip-on gauge and devices for the execution of the test.

A clip-on gauge is used to measure the horizontal displacement of the two points immediately over the notch during loading; the displacement is applied with controlled rate; it means that, once established the amount of opening to realize per second, the machine modulates its rate according to the noticed resistance, incrementing or decreasing the force on the crack. The maximum value of the crack mouth opening has to be defined in order to set-up a condition for ending the test. One way to do so is to refer to the Eurocode 2: it establishes that the CMOD value of 400 μm can be considered the discriminating threshold between an acceptable and an unacceptable crack width in serviceability limit state for non aggressive exposure conditions [18]. Thus, if a bigger value is chosen, it will have the aim to emphasize the effect of the damaging action on the overall mechanical and durability properties of the element tested.

– In load control:

The test is performed on specimens without a notch. It consists into the application of an increasing load with a constant rate. The crack width is neither measured nor controlled during the test. In this condition, the stress state at the tip of the crack is always maintained by the imposed load [19].

Recently, to improve the stability of the two halves after the fracture, it has been demonstrated that a carbon fibre reinforced polymer strip can be applied over the specimen before the start of test, forbidding the complete separation of the two halves of the specimen after failure and their relative rotation around their longitudinal axis. In this way, the stability of the system after cracking is guaranteed despite the absence of specific crack opening control during the test [1].

Three considerations are necessary in both configurations: the first one is that the crack opening is measured relating two points immediately over the notch during the test while as the average of the crack opening in different chosen random locations for the analysis [3]; the second is that when the maximum crack width is reached, the specimen is gradually unloaded through an inversion of the movement of the piston: the effect is a partial closure of the crack; the last one is that after the fracture, the specimen is removed from the loading frame and stored in a controlled environment for a period necessary for the self-healing reactions to be established. The result is expressed in form of a cartesian chart whose axes are, for example, the variables load applied/crack displacement. According to the typology of selected test, the curve will provide different information [13]; in fact in case of a test in load control the specimen shows an approximately elastic and linear behaviour until a certain level, after which there is a sudden drop in load that corresponds to the failure of the specimen; on the contrary, if the test is in deformation control, the behaviour of the specimen can be investigated and plotted also after the cracking phase. This part of the curve represents the softening of the material. These considerations are in general valid and well distinguishable for tests performed on the samples without capsules. For specimens with embedded macrocapsules, further reflections must be made; regarding to the initial elastic part of the loading phase, this is not perfectly linear because the heterogeneities of the matrix create unevenness of the stresses, producing the system response with different stiffnesses. Instead, for what concerns the softening part, it is possible to notice that localized vertical drop are measured when the break of the capsules occurs; in fact, shells represent the most rigid part of the system when the matrix already shows a fracture; when they break there is an immediate fall of the curve. In reality, vertical falls can be also related to the break of already hardened polyurethane on shells walls. Finally, a consideration concerns test setting in terms of rate applied: it is evident that the chosen value is different for

the encapsulated samples and the nonencapsulated ones because for the latter their homogeneous matrix does not create problem on the test control. In the paragraphs below, the results and the comparisons between the encapsulated specimens and the nonencapsulated ones are listed for each series, specifying also for each one the test conditions.

2.3.1.1. Setup, results and outcomes for A_CAP

The test has been realized with the following settings:

- Typology test: CMOD;
- Notch dimensions (casted): 4 mm by 4 mm;
- Maximum crack width: 800 μm ;
- Deformation rate (for CAP): 1,5 $\mu\text{m/s}$;
- Deformation rate (for REF): 3 $\mu\text{m/s}$;
- Temperature value: room temperature ($20 \pm 2^\circ\text{C}$).

Results are now reported in the **Figures 2.5** and **2.6**. below in terms of load applied/extensometer displacement both for CAP and REF ones.

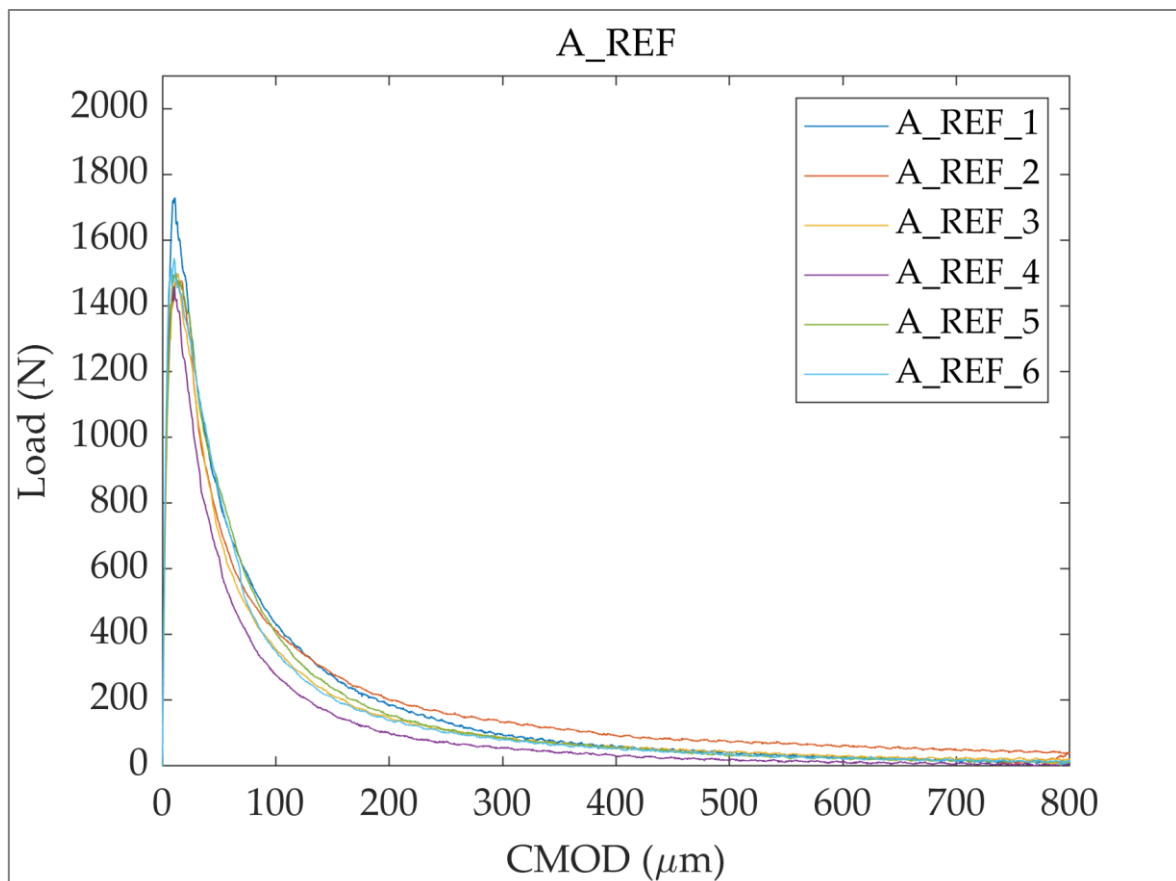


Figure 2.5. Results of the pre-cracking test for A_REF samples.

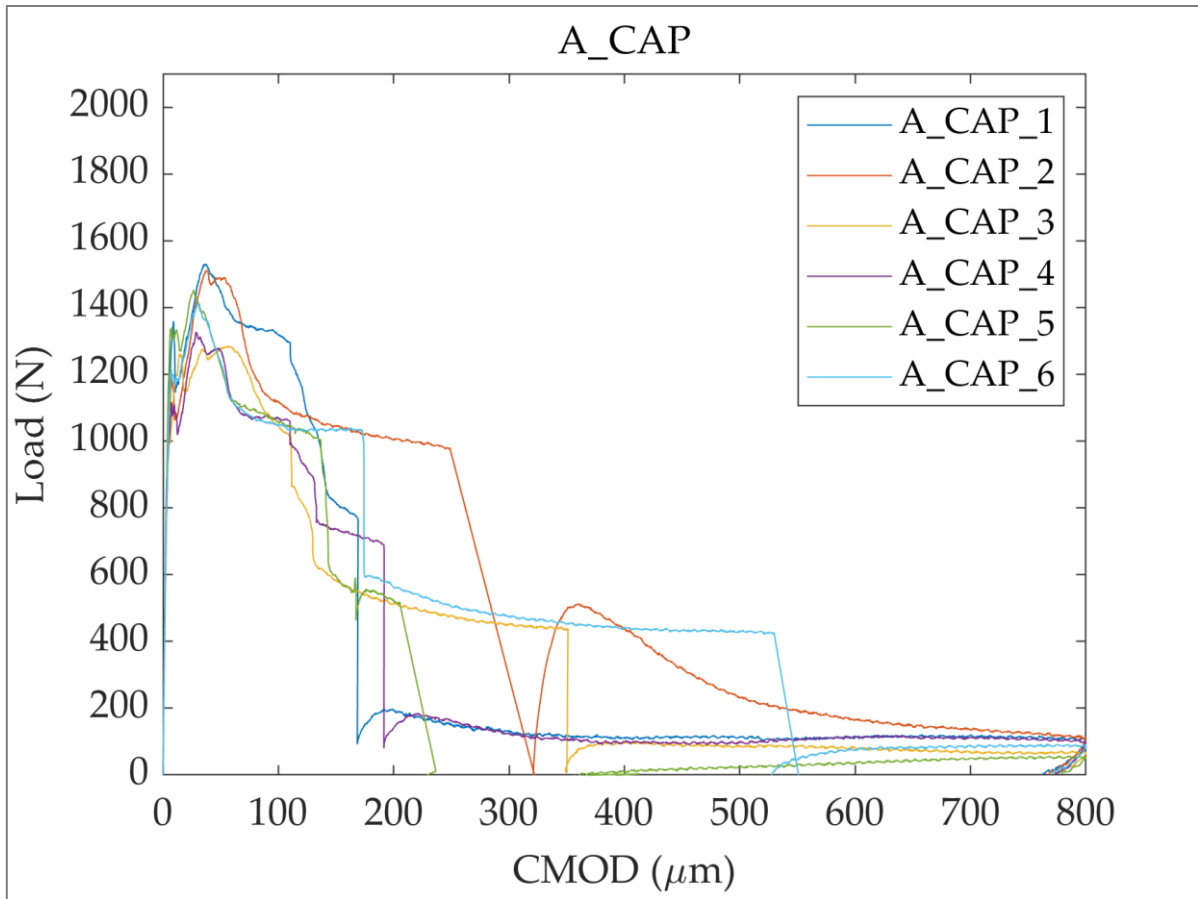


Figure 2.6. Results of the pre-cracking test for A_CAP samples.

It is reported that during the execution of the tests, some problems occurred for the specimens A_CAPS_2, A_CAPS_5 and A_CAPS_6. In detail, after the break of the capsules, the testing machine showed technical troubles and, for this reason, the specimens have been unloaded and even the acquisition of the data was stopped. Subsequently, they have been reloaded again until the crack width reached the chosen value. Nonetheless, it is believed that the results obtained are valid.

For all the specimens, after the break of the capsules, the core has been released, forming a polyurethane foam with a compact alveolar structure. Probably, this aspect will have a positive impact on the results of the durability tests.

2.3.1.2. Setup, results and outcomes for B_CAP

The test has been realized with the following settings:

- Typology test: CMOD;
- Notch dimensions (casted): 4 mm by 4 mm;
- Maximum crack width: 800 μm ;
- Deformation rate (for CAP): 1,5 $\mu\text{m/s}$;
- Deformation rate (for REF): 3 $\mu\text{m/s}$;
- Temperature value: room temperature ($20 \pm 2^\circ\text{C}$).

Results are now reported in the **Figures 2.7** and **2.8** below in terms of load applied/extensometer displacement both for CAP and REF ones.

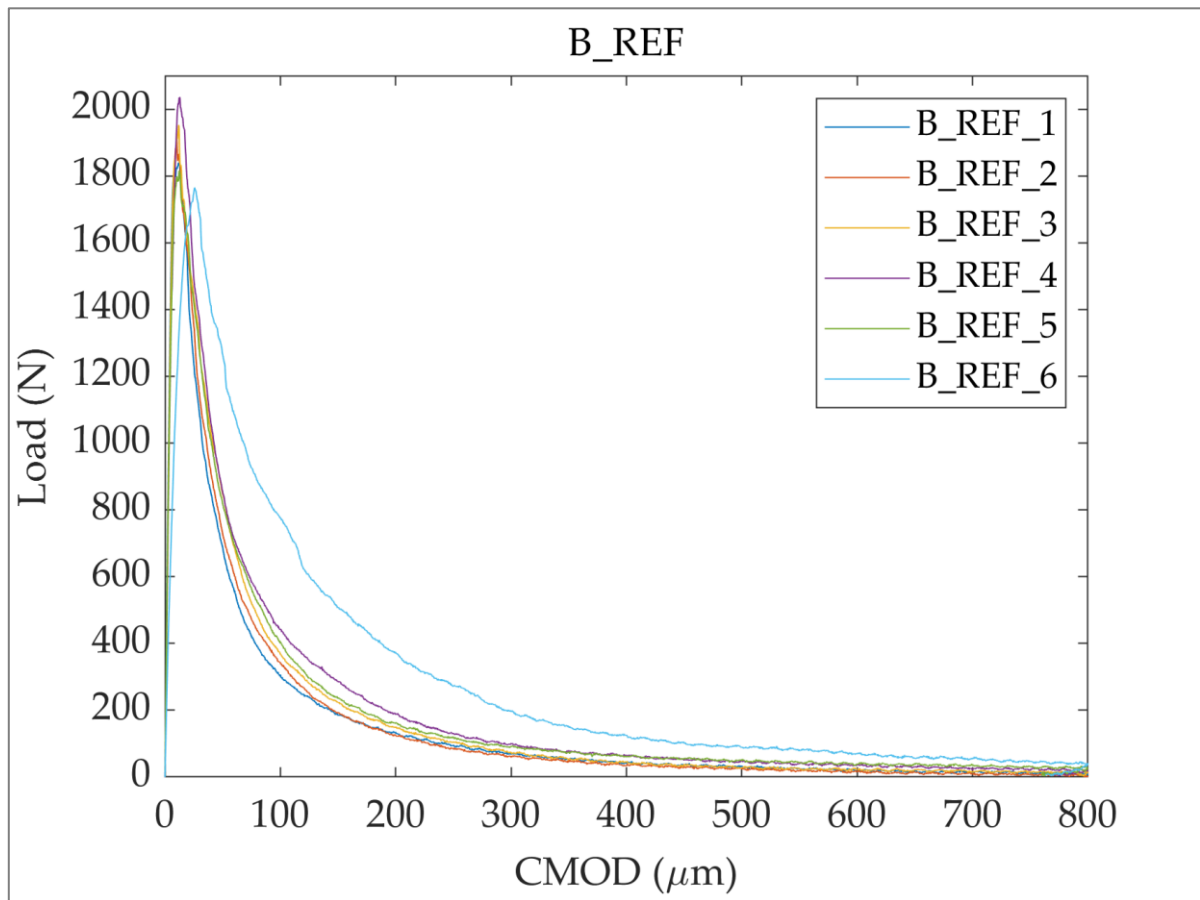


Figure 2.7. Results of the pre-cracking test for B_REF samples.

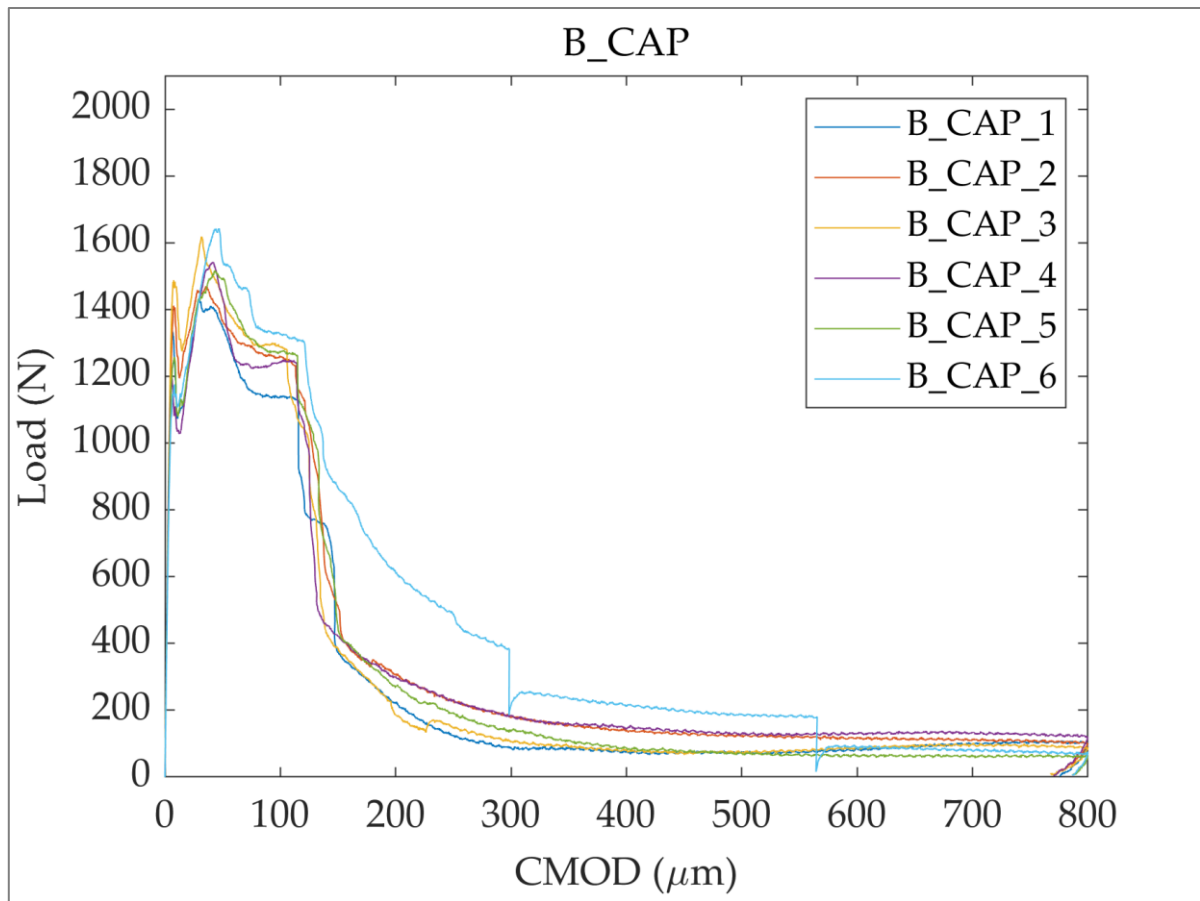


Figure 2.8. Results of the pre-cracking test for B_CAP samples.

.For this series, no drawbacks happened during the execution of the test. The leakage of the polyurethane happened naturally, without problems.

2.3.1.3. Setup, results and outcomes for RRT5

The test has been realized with the following settings:

- Typology test: test in load control;
- Notch dimension: absent;
- Maximum crack width: 400 μm ;
- Load rate: 50 N/s;
- Temperature value: room temperature ($20 \pm 2^\circ\text{C}$).

For this series, after the acquisition of the data, there was not the plotting of the results. In any case, no drawbacks happened during the execution of the test. The leakage of the polyurethane happened naturally, without problems. About the geometry of the crack: the absence of the notch allows the creation of a crack path more tortuous but, at the same time, more natural.

Immediately after cracking, the specimens were placed with their crack mouth facing upwards and the crack width was restrained using screw jacks to approximately 300 μm . The crack width was then further restrained under an optical microscope using an iterative procedure of measuring and restraining. The specimens were then turned so that the crack mouth was facing downwards (i.e. CFRP facing upwards) [1].

2.3.1.4. Setup, results and outcomes for CCAP_S

The test has been realized with the following settings:

- Typology test: test in load control;
- Notch dimension: absent;
- Maximum crack width: 400 μm ;
- Load rate: 50 N/s;
- Temperature value: room temperature ($20 \pm 2^\circ\text{C}$).

For this series, after the acquisition of the data, there was not the plotting of the results. In any case, no drawbacks happened during the execution of the test. The leakage of the polyurethane happened naturally, without problems.

Immediately after cracking the specimens were placed with their crack mouth facing upwards and the crack width was restrained using screw jacks up to a target crack width of 300 μm [1].

2.3.1.5. Setup, results and outcomes for CCAP_L

The test has been realized with the following settings:

- Typology test: test in load control;
- Notch dimension: absent;
- Maximum crack width: 400 μm ;
- Load rate: 50 N/s;
- Temperature value: room temperature ($20 \pm 2^\circ\text{C}$).

For this series, after the acquisition of the data, there was not the plotting of the results. In any case, no drawbacks happened during the execution of the test. The leakage of the polyurethane happened naturally, without problems.

Immediately after cracking the specimens were placed with their crack mouth facing upwards and the crack width was restrained using screw jacks up to a target crack width of 300 μm [1].

2.3.2. Experimental details for Water Flow test

The durability of the sealed specimens was evaluated with a Water Flow Test. During the years, several configuration and technical settings were defined to properly execute this test [3]. It is now reported a general description of the method proposed by the SARCOS Protocol.

Before the execution of the test, specimens were stored dry in an indoor climate with their crack facing downwards for at least 1 day to allow that the healing agent reaches a chemically settle. Afterwards, specimens were submersed in demineralized water for 24 to 48 hours to prevent any influences on the results related to the water absorption by the matrix, namely to ensure that the water subsequently injected would cross the specimen avoiding the dispersion inside the matrix, already saturated, as shown in **Figure 2.9**.

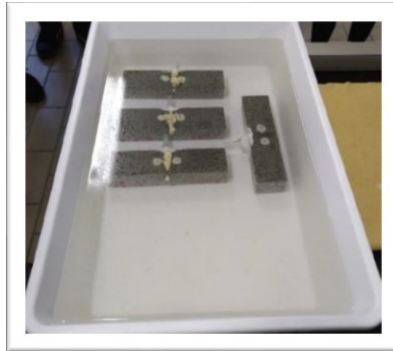


Figure 2.9. Submersion of specimens for the preparation to the water flow test.

The specimens were then taken out of the water and were surface dried. To connect the specimens to the water flow setup, a short tube was then inserted in the cast-in hole and a watertight connection was ensured using silicone. The other side of the cast-in hole was sealed completely with silicone; these additions were realized during the casting of the specimens, that is before the realization of the pre-cracking test. The inserted tube was then connected to a tube in contact with an open water reservoir, as shown in **Figure 2.10**. In case of absent cast-in hole, the tube is directly connected with the specimen, applying it on its crack edge, after rotating the specimen of 90 degrees, via small funnel covering the entire crack length.



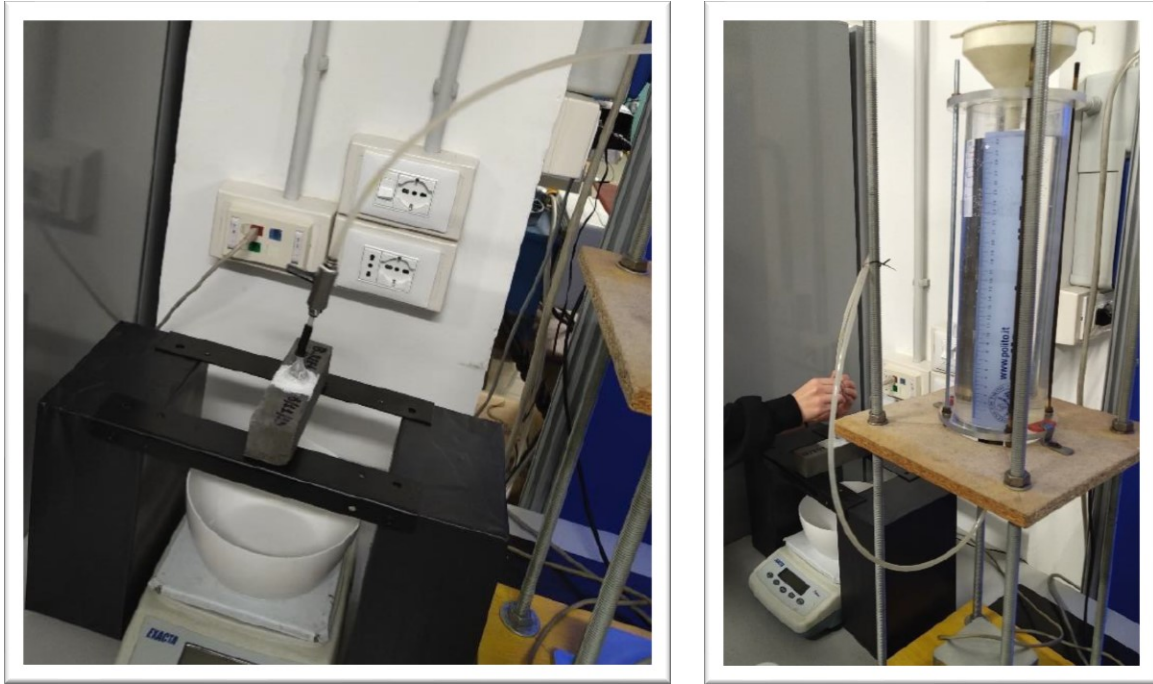


Figure 2.10. Setup for the connection of, respectively, self-healing and reference specimen to the water reservoir.

The water head, measured from the tube in the specimens up to the water level, was kept constant throughout the test at 50 ± 2 cm by topping up with demineralized water whenever required, as shown in **Figure 2.11**; the aim was to ensure a constant water pressure.

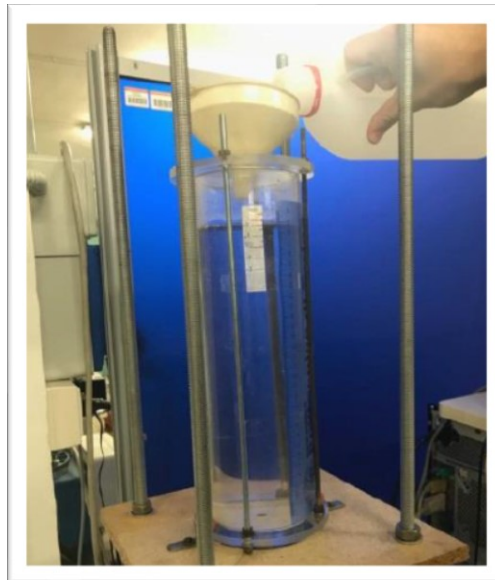


Figure 2.11. Filling of the water reservoir to provide a constant pressure to the sample.

Water from the reservoir flowed through the tubes into the cast-in hole, from where it could leak out of the specimens via the crack. Only the water that leaked out of the crack mouth, i.e. the bottom side of the specimens, was considered. Therefore, the sides of the specimens were

sealed prior to saturation by using aluminium tape, silicon sealant, or a viscous glue (e.g. viscous methyl methacrylate). It is important to provide a perfect sealing of a certain area around the crack to be sure that the water is perfectly canalized inside the sealed fracture. An example of isolation of a specimen is provided in **Figure 2.12**.

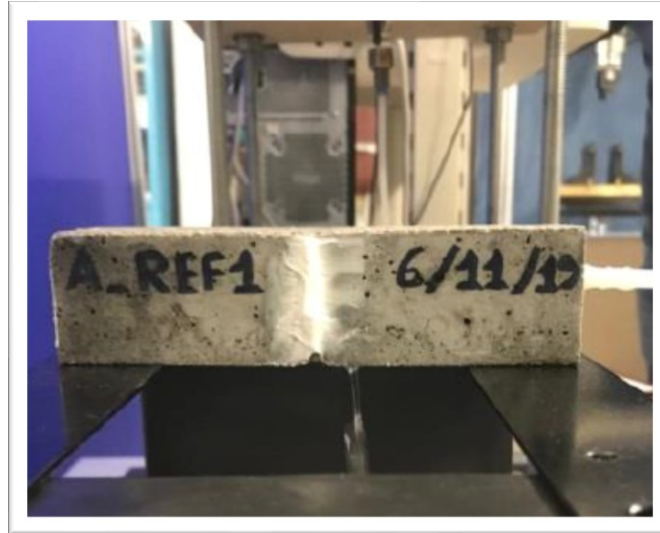


Figure 2.12. Isolation of crack.

The first 60 s that water leaked from the crack were discarded in order to measure only a fully developed flow and to allow water bubbles to be flushed from the system. Subsequently, the weight of the water which leaked from the crack was recorded for a minimum of 6 min. The flowed water was measured recording the water collected in a container placed under the specimens through a balance, see **Figure 2.13**.



Figure 2.13. Registration of water passed through the crack.

A schematic representation of the setup is provided in **Figure 2.14**.

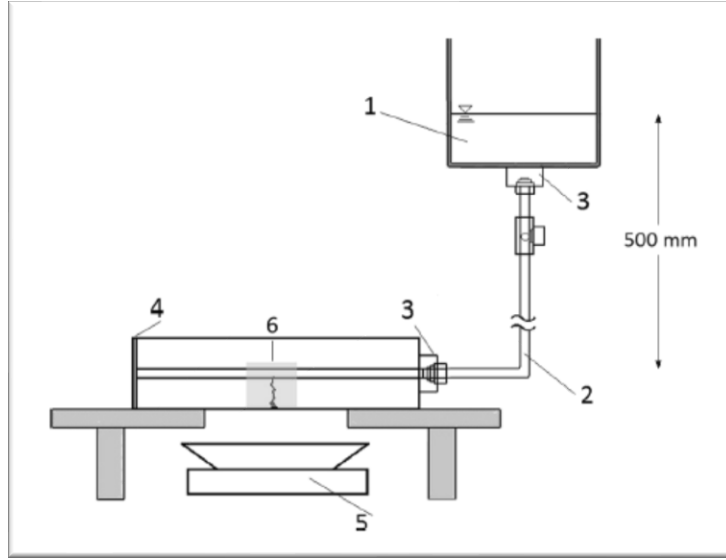


Figure 2.14. Schematization of test setup [3].

If the effect of the healing system is positive, the amount water passed through the specimens should be negligible than that recorded for the non-encapsulated ones. For this reason, the sealing efficiency SE_{flow} of CAPS specimens with respect to REF specimens can be calculated through the Expression (2):

$$SE_{flow} = \frac{\bar{q}_{REF} - \bar{q}_{CAPS}}{\bar{q}_{REF}} \quad (2)$$

Where

- \bar{q}_{REF} represent the water flow (g/min) of the reference specimens;
- \bar{q}_{CAPS} represents the water flow (g/min) of the self-healing specimens containing capsules;

Where

- \bar{q}_{REF} is calculated by the ratio between the mass variation of the reference specimens during the 6 minutes and the duration time of the test;
- \bar{q}_{CAPS} is calculated by the ratio between the mass variation of the self-healing specimens during the 6 minutes and the duration time of the test.

2.3.2.1. Results and outcomes for A_CAP

The results obtained for this series are summarized in **Figure 2.15**:

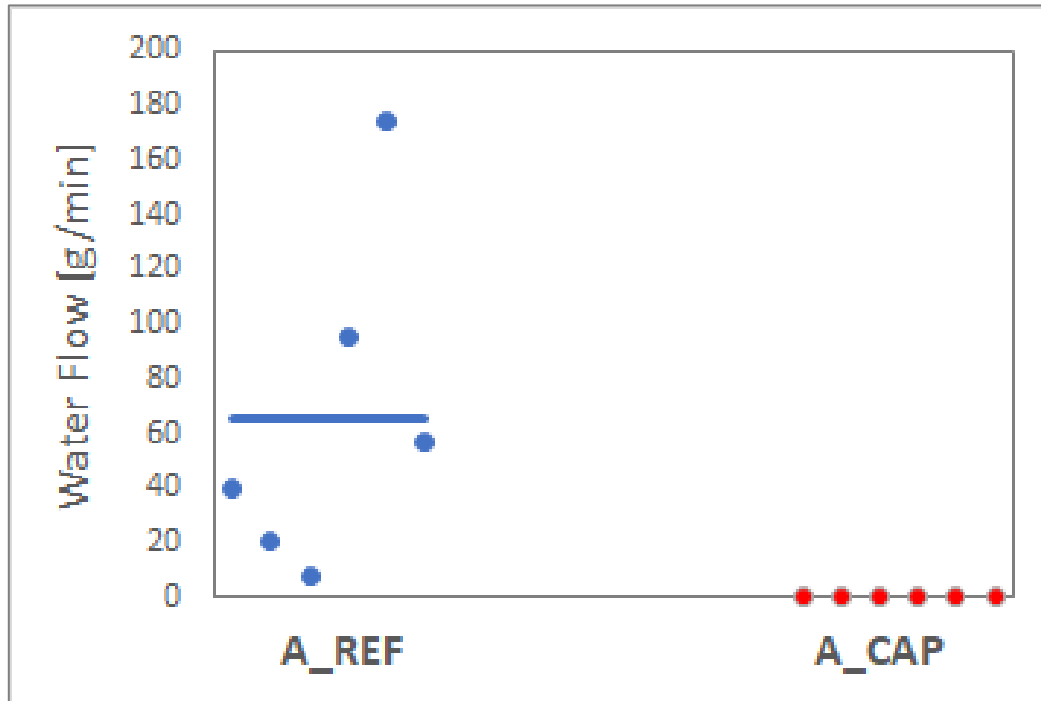


Figure 2.15. Result of water flow test for A_CAP and A_REF series.

From the results, it is clear that for all specimens the efficiency of the self-healing system is equal to 100%. This means that the healing agent has completely closed the crack, isolating the specimens from the exterior. In fact, a different behaviour is shown by the cracked specimens used as reference: for them, the amount of water passed through is not negligible.

A notable aspect is the reaction to the test of the specimens A_REF_4 and A_REF_5: at a certain point the water started also to leak from the upper surface, sign that they were completely cracked.

2.3.2.2. Results and outcomes for B_CAP

The results obtained for this series are summarized in Figure 2.16:

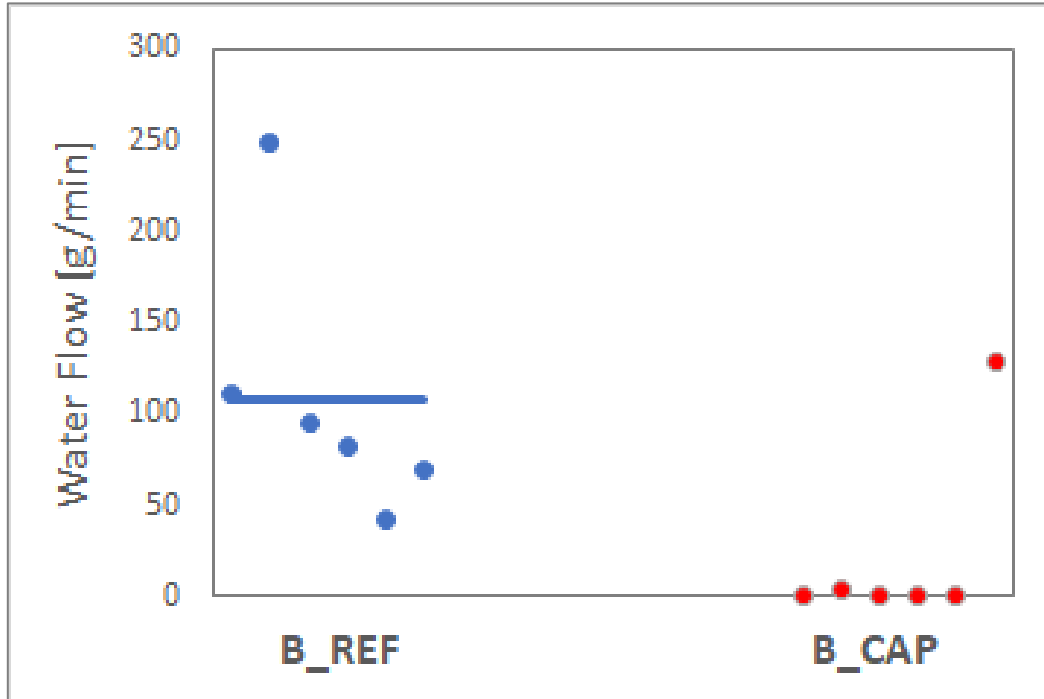


Figure 2.16. Result of water flow test for B_CAP and B_REF series.

Because this series has not the cast-in holes for the test, the tube connected to the reservoir is directly applied on the crack edge after rotating the specimen of 90 degrees, via small funnel covering the entire crack length. In this way, the water provided by the reservoir after opening the hydraulic circuit could find a way out through the edge of the crack (which is at the bottom of the specimens in this water flow setup) and through the crack mouth (which is at the side of the specimen in this water flow setup). Therefore, a more severe bidirectional water flow setup is achieved, to complete the experimental data obtained through the unidirectional water flow setup described in *Paragraph 2.3.2*. From the results, it is clear that for 5 of 6 specimens the efficiency of the self-healing system is equal to 100%. This means that the healing agent has completely closed the crack, isolating the specimens from the exterior. In fact, a different behaviour is shown by the cracked specimens used as reference: for them, the amount of water passed through is not negligible.

A notable aspect is the reaction to the test of the specimens B_REF_2 and B_CAP_6: for the former, at a certain point the water started also to leak from the upper surface, sign that it was completely cracked, thus the test was stopped before the conclusion of the 7 minutes because

the basin was already entirely full; for the latter, the amount of water passed was too high and the sample received no improvement from the presence of the capsules: it is probable that the healing agent did not leak, resulting pointless. From a statistical point of view, the value of WF for B_CAP_6 is inconsistent, showing a higher flow than the average of the series.

2.3.2.3. Results and outcomes for RRT5

The results obtained for this series are summarized in **Figure 2.17**:

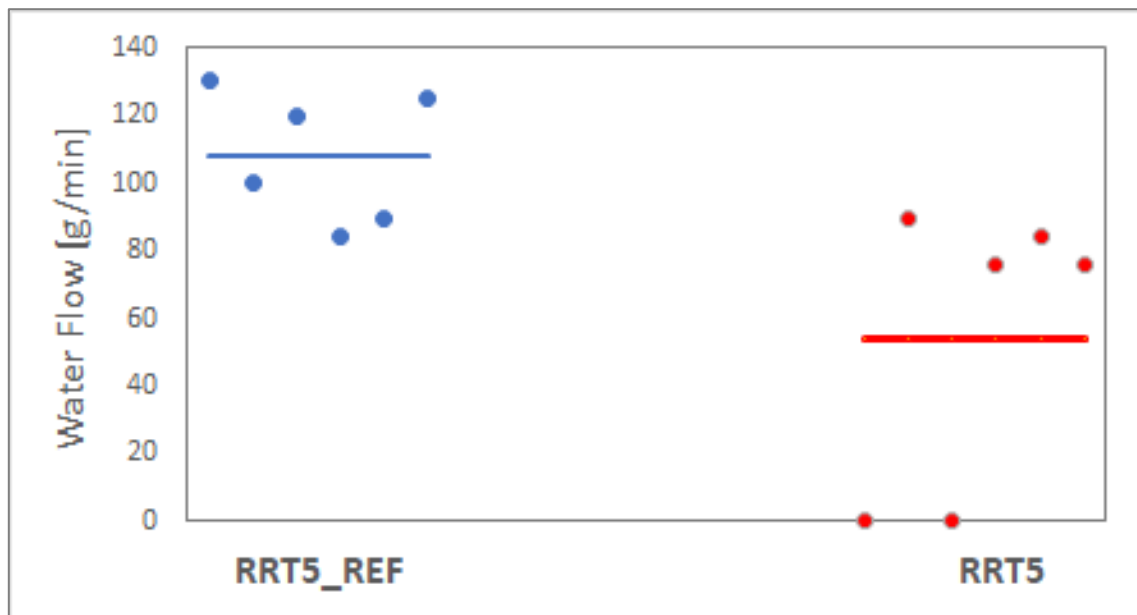


Figure 2.17. Result of water flow test for RRT5 and RRT5_REF series.

The results for this series have been produced by different laboratories because, in reality, these samples are part of a wider research project conducted at European level.

In general, both the reference and the self-healing specimens show a high variation of the water flow. For the former, it could depend on the crack tortuosity; for the latter, it has been demonstrated that it depends on the outflow of the polyurethane. In detail, sectioning a sample after the test, it was seen that only a small part of the healing agent sealed the crack while the remaining part polymerized inside the capsule. For all these aspects, the results of all laboratories outline the same tendency: the sealing efficiency is promising but definitely not perfect.

2.3.2.4. Results and outcomes for CCAP_S

The results obtained for this series are summarized in **Figure 2.18**:

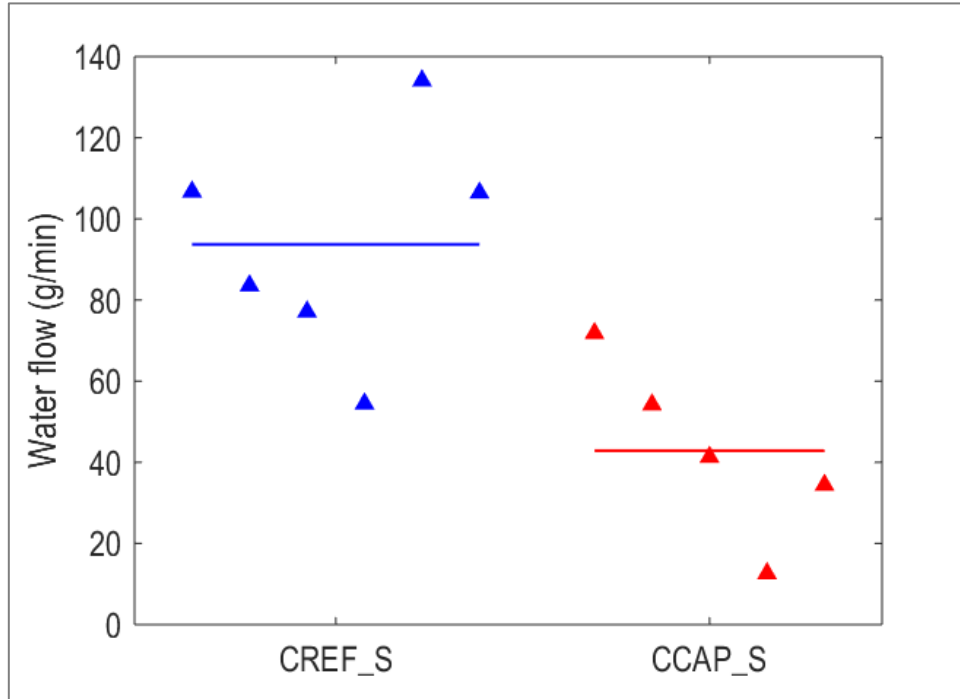


Figure 2.18. Result of water flow test for CCAP_S and CREF_S series.

The self-healing specimens showed a water flow lower than that of the corresponding reference specimens. During the test, a dripping behaviour was manifested by CAP while a steady flow by the reference specimens. In general, a satisfactory sealing efficiency was assessed, but that is lower and with a higher variability if compared to that of the large capsule specimens of the series CCAP_L. This could be possibly ascribed to a lower release of healing agent. A more detailed investigation, for example through the sectioning of the specimens, can be performed, in order to detect the cause.

2.3.2.5. Results and outcomes for CCAP_L

The results obtained for this series are summarized in **Figure 2.19**:

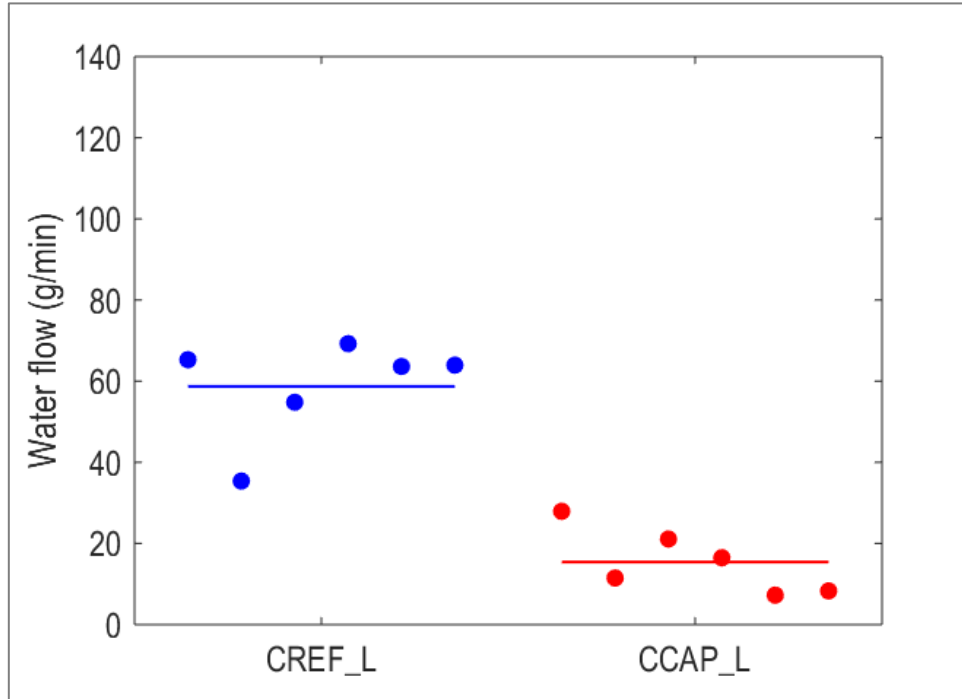


Figure 2.19. Result of water flow test for CCAP_L and CREF_L series.

For this series a low water flow was measured; this is absolutely a sign of a good release of polyurethane from these specimens. In the majority of the self-healing specimens just a constant slow dripping was visible. As might be expected, the dripping was visible just from the zone of the crack that was not covered by the polyurethane. Definitely, a good sealing efficiency was obtained of almost all the samples with respect to the reference specimens, showing an important property: a relatively low variability.

2.3.3. Experimental details for Mechanical Reloading

A test that generally is used for a last survey of specimens is the mechanical reloading. It expresses the recovery of load-carrying capacity under mechanical test, that usually is the same used for the pre-cracking stage [3]. It consists in the reloading of the healed specimens but also, when it is physically possible, of the reference ones. In this way, the efficiency of the healing systems is evaluated in terms of recovery of strength and stiffness. Some authors proposed in literature [3] expressions (4), (5), (6) for the calculation of indices related to the recovery of, respectively, the residual post-cracking load bearing capacity, stiffness, “equivalent” crack closure; these are:

$$- \text{ Index of load recovery: } ILR = \frac{P_{max,reloding} - P_{unloading}}{P_{max,uncracked} - P_{unloading}} \quad (4)$$

Where

- $P_{max,reloding}$ is the peak load obtained during the re-loading stage;
- $P_{max,uncracked}$ is the peak load reached during the pre-cracking stage;
- $P_{unloading}$ is the residual load obtained at the moment of unloading preceding the reloading stage;

$$- \text{ Index of damage recovery: } IDR = \frac{K_{reloding} - K_{unloading}}{K_{loading\ uncracked} - K_{unloading}} \quad (5)$$

$$- \text{ Index of crack healing: } ICH = \frac{\text{crack closure}}{\text{initial crack opening}} \quad (6)$$

From a practical point of view, the test consists in the application of a load till the rupture of the specimen, as shown in **Figure 2.20**. The cases analysed in these tests had all a pre-cracking through three-point bending test. Thus, the failure of all these series was realized with this flexural test.



Figure 2.20. Failed self-healing and reference specimens.

2.3.3.1. Results and outcomes for A_CAP

The results are reported in **Figures 2.21** and **2.22** below, in terms of applied load/displacement of the extensometer. While the test was always conducted for the specimens of the series CAP, reference samples were led to breakage only if they were partially cracked from the pre-cracking test. The average LRI of reloaded self-healing specimens was 87%, while the reference samples did not show any mechanical recovery.

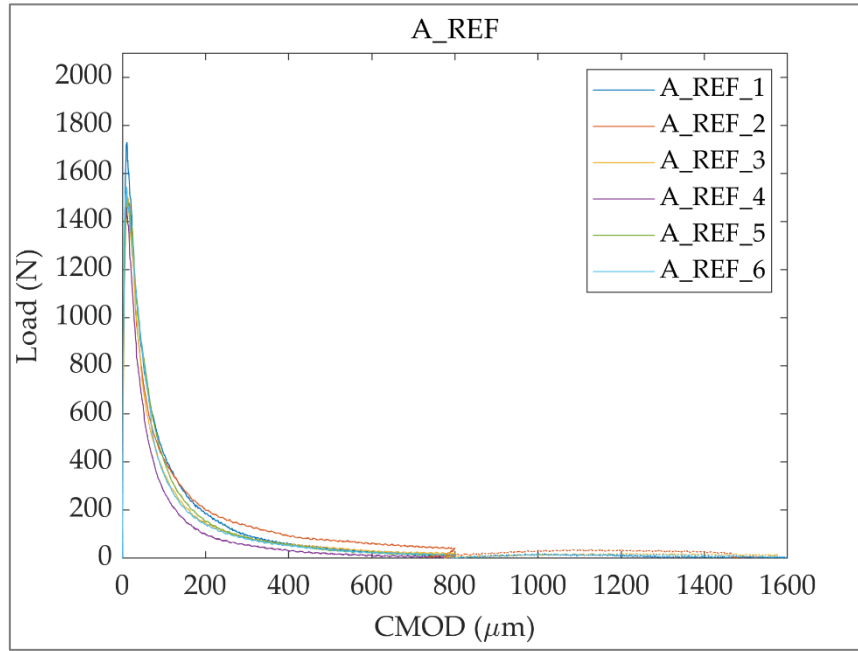


Figure 2.21. Results of the pre-cracking test for A_REF samples.

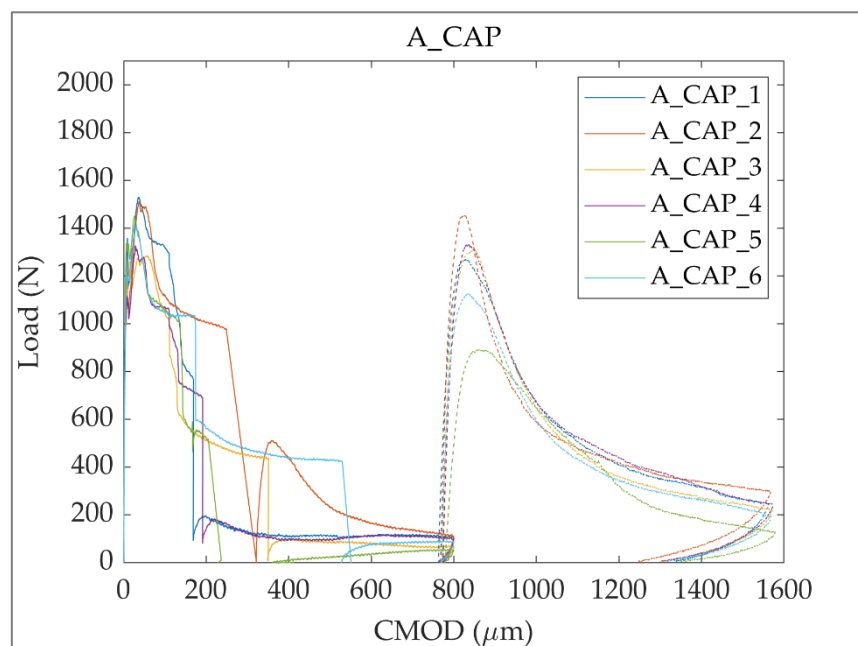


Figure 2.22. Results of the pre-cracking test for A_CAP samples.

A total recovery was reached by the specimens A_CAP_2, A_CAP_3, A_CAP_4; optimal results also for the specimens A_CAP1 and A_CAP6. The worst recovery was shown by the specimen A_CAP_5, that was the only sample with the lowest value of LRI, but always with a positive sign. Definitely, it is evident that in the pre-cracking stage the presence of capsules has not a negative effect on the peak load, that is they do not alter negatively the mechanical characteristics of the matrix in that phase. An important aspect to underline is that, in general, the part of curve relative to the softening behaviour, at this stage, is improved; it means that after the peak, there is not an almost instantaneous fall of the load but the system shows a more ductile response to the load increase. Moreover, it is reported that for specimens A_REF_4 and A_REF_5 the reload test was impossible to realize because they were completely cracked already from the pre-cracking step. All data are summarized in **Figure 2.23**.

Sample	Peak Load Pre-cracking [N]	Peak Load Post-cracking [N]	ILR [%]
A_CAP_1	1531	1270	81.7
A_CAP_2	1511	1453	95.8
A_CAP_3	1285	1311	102.1
A_CAP_4	1326	1332	100.5
A_CAP_5	1452	893	60.0
A_CAP_6	1419	1127	78.4
A_REF_1	1729	21	0.6
A_REF_2	1476	37	-0.13
A_REF_3	1498	22	0.14
A_REF_4	1459	NaN	NaN
A_REF_5	1501	NaN	NaN
A_REF_6	1545	20	0.23

Figure 2.23. Peak load data of flexural tests for the series A_CAP and its REF.

2.3.3.2. Results and outcomes for B_CAP

The results are reported in **Figures 2.24** and **2.25** below, in terms of applied load/displacement of the extensometer. While the test was conducted for the specimens of the series CAP, reference samples were led to breakage only if they were partially cracked by the pre-cracking test. The average LRI of reloaded self-healing specimens was 61%, while the reference samples did not show any mechanical recovery.

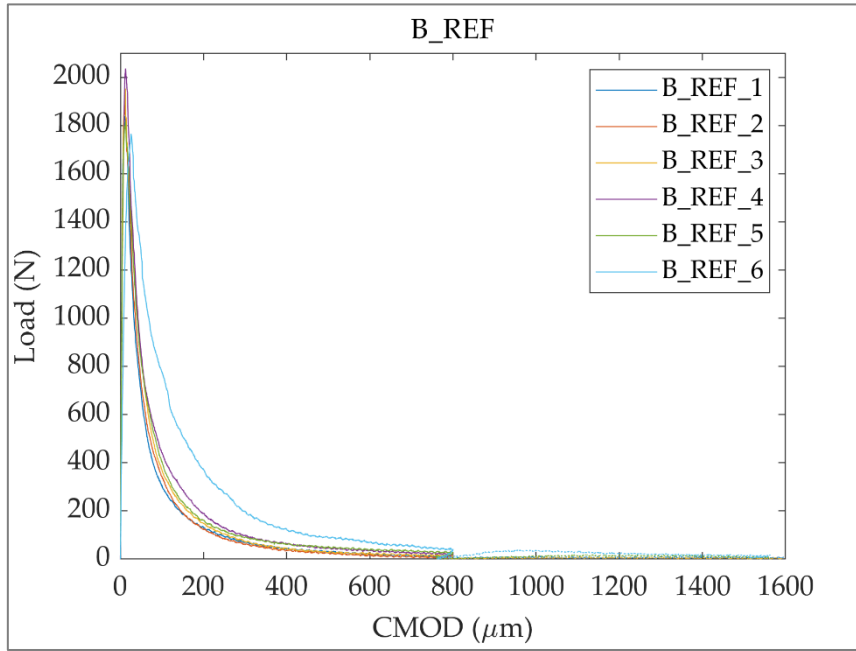


Figure 2.24. Results of the pre-cracking test for B_REF samples.

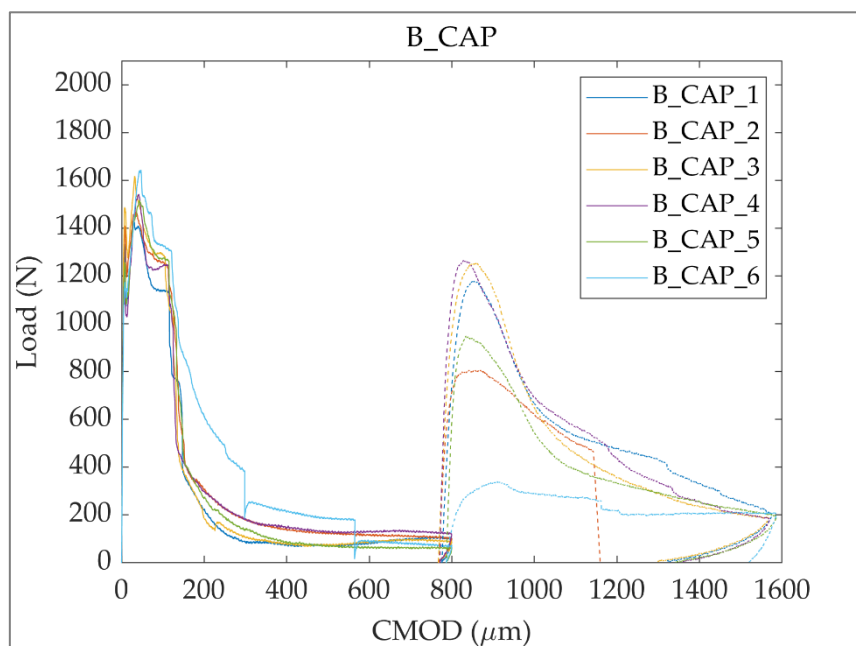


Figure 2.25. Results of the pre-cracking test for B_CAP samples.

A total recovery was reached by the specimens A_CAP_1, A_CAP_3, A_CAP_4; optimal results also for the specimens A_CAP_2 and A_CAP_5. The worst recovery was shown by the specimen A_CAP_6, that was the only sample with the lowest value of LRI. Definitely, it is evident that in the pre-cracking stage the presence of capsules has not a negative effect on the peak load, that is they do not alter negatively the mechanical characteristics of the matrix in that phase. An important aspect to underline is that, in general, the part of curve relative to the softening behaviour, at this stage, is improved; it means that after the peak, there is not an almost instantaneous fall of the load, but the system shows a more ductile response to the load increase. Moreover, it is reported that for specimens A_REF_2 and A_REF_4 the reload test was impossible to realize because they were completely cracked already from the pre-cracking step. All data are summarized in **Figure 2.26**.

Sample	Peak Load Pre-cracking [N]	Peak Load Post-cracking [N]	ILR [%]
B_CAP_1	1429	1178	81.1
B_CAP_2	1470	806	51.5
B_CAP_3	1617	1254	76.2
B_CAP_4	1541	1265	80.6
B_CAP_5	1516	948	60.9
B_CAP_6	1643	340	17.1
B_REF_1	1839	13.17	0.2
B_REF_2	1909	NaN	NaN
B_REF_3	1952	11.5	-0.09
B_REF_4	2035	NaN	NaN
B_REF_5	1816	19	-0.35
B_REF_6	1765	38.9	-0.15

Figure 2.26. Peak load data of flexural tests for the series B_CAP and its REF.

2.3.3.3. Results and outcomes for RRT5

This test was not executed for this series.

2.3.3.4. Results and outcomes for CCAP_S

This test was not executed for this series.

2.3.3.5. Results and outcomes for CCAP_L

This test was not executed for this series.

3. Calculation of the spreading area of the healing agent

Some authors in their projects [3], [5], [9] tried to find a correlation between the mechanical strength and stiffness recovery with the area covered by healing agent. This analysis was possible thanks to the acquisition of images of all the samples containing the capsules after the complete failure by means of a digital camera. The images were processed and corrected of their optical defects; finally, the definition of the spreading region of the healing agent was achieved. Starting from these results, the purpose of this thesis is to define an algorithm for the digital calculation of the expansion area of the healing agent; the idea is to evaluate visually the spreading to gain qualitative information about the filling of the cracks and the effects of the agent on the improvement of mechanical and physical properties of the maintained samples. Indeed, this type of analysis represents a completion of the tests realized before and described in *Chapter 2*; in fact, an investigation of this kind can be considered probably the most immediate and automatic to be conducted [3]. In reality, only correlating the values of area with other properties (for example, with the results of the durability tests or with other geometric properties) it can be decided if this kind of parameter is functional or not to the evaluation of the healing system.

The proposed procedure for the calculation of the spreading area is now reported and explained for only one specimen; in fact, the considerations must be considered valid for all the other samples of all the other series. In sake of simplicity, the specimen used to illustrate the process is one of the series RRT5: in this case, the colour contrast between the matrix and the healing agent is maximum thanks to the addition of a fluorescent powder to the polyurethane before the casting of the capsules, as described in *Paragraph 1.2.4*. The computation consists essentially in two steps: the first one subsists in the correction of optical details of the digital images acquired by GIMP, while the second one involves the individuation and quantification of the area by IMAGEJ.

3.1. Digital corrections on GIMP

In this phase, the idea is to correct all the defects that the images show; they can consist in problems of distortion, orientation, sharpness, saturation and so on. In this work, the Open Source Image Editor GIMP (v. 2.10.18) was used. The GNU Image Manipulation Program (GIMP) is a cross-platform image editor for such tasks as photo retouching, image composition and image authoring [14]. The incidence of the digital manipulation, obviously, depends on the

accuracy of the photos taken (focus, exposure, ...). However, the employ of an image editor is essential for the achievement of the final copy of the surface to be analysed on IMAGEJ.

The starting point of this phase is the image of the specimen after the reloading step or, more in general, when it has come to break. Thus, the editing begins from the photo of the two juxtaposed surfaces of the broken specimen, covered by the healing agent leaked during the pre-cracking and reloading tests, as shown in **Figure 3.1**.



Figure 3.1. Starting image of the broken specimen.

The procedure used to adjust all the fine details of the photo consists in several points, concerning:

- Separation of images of the surfaces on two layers (**Figure 3.2**):
the two surfaces are carried on two different layers; in fact, during the editing, they will be corrected separately, according to their defects.

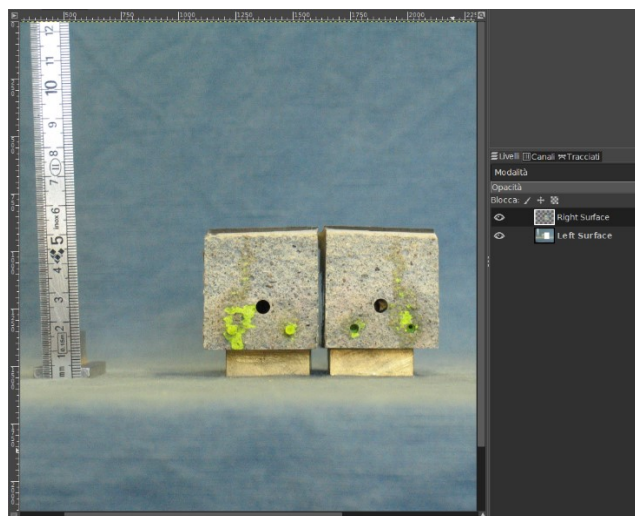


Figure 3.2. Creation of two layers.

– Correction of the distortion (**Figure 3.3**):

the photo's perspective must be adjusted; this correction refers to all the problems related to the apparent inclination of the sides of the objects that makes their corners look not perfectly perpendicular. This imperfection is due to the perspective from which the photo was taken. The application of the *Perspective Tool* needs the definition of guidelines as references. This tool has to be applied to the surfaces in subsequent stages. The correction is considered adequate when the surface is square, namely when the vertices of the object are ideally orthogonal.

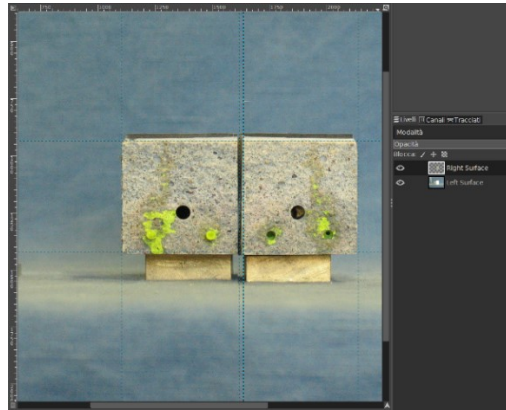


Figure 3.3. Correction of photo's perspective.

– Correction of the scale of the image (**Figure 3.4**):

the two surfaces are now scaled using as reference quantity the width of the specimen; in fact, the surfaces are ideally considered square but, in reality, their geometry is not so defined. This aspect is a natural consequence of the handmade casting; despite the maximum accuracy during the process, some mistakes can be made. For this reason, the dimension of the specimen that is certainly comparable is the width instead of the height. Note that this geometric parameter remains the reference quantity more reliable of the image: despite of the presence of a graduated rod in photo, this is not used to scale the image. In fact, it is probable that the crack faces and the rod do not lay on the same geometric plane.

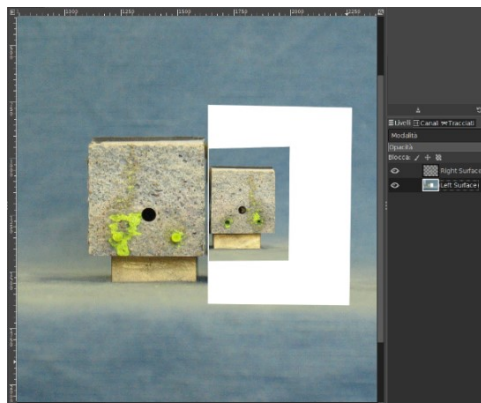


Figure 3.4. Application of the scale layer Tool.

- Overturning of one surface (**Figure 3.5**):
in order to correctly overlap the surfaces for the final result, one of them needs to be overturned; for this purpose, the *Flip Tool* is used.

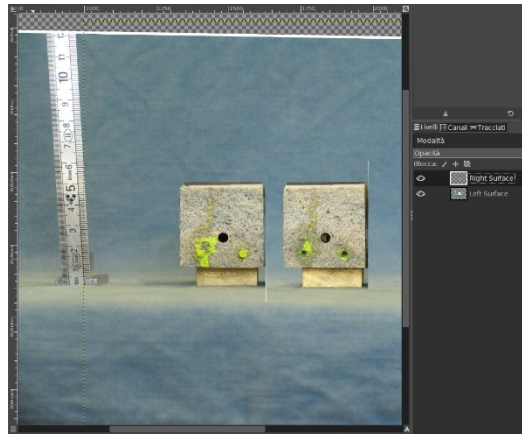


Figure 3.5. Overturning of the left surface.

- Correction of colour contrast (**Figure 3.6**):
the aim of this step is to enhance the colour contrast between the matrix and the healing agent to simplify its individuation on IMAGEJ. For this reason, the change of saturation and exposure level through the *Menu Colours* is necessary.

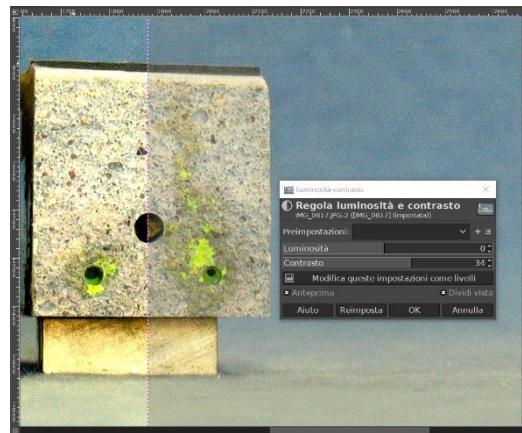


Figure 3.6. Regulation of the levels of saturation.

- Overlapping of the surfaces (**Figure 3.7**):
in order to overlap the two surfaces, as first step, the alignment is realised. The reference points are the capsules and the central hole of the specimen. This step requires high precision; thus, to simplify the process the opacity of the upper layer can be decreased. Once the two surfaces are combined in only one image, the *Layer Mode* is converted in *Lighten only Mode*; this mode compares each pixel of a layers with the corresponding one on the other and it uses the larger value in the resulting image; it is a commutative

mode, namely the definition of the upper and the lower layer does not influence the final result [14].

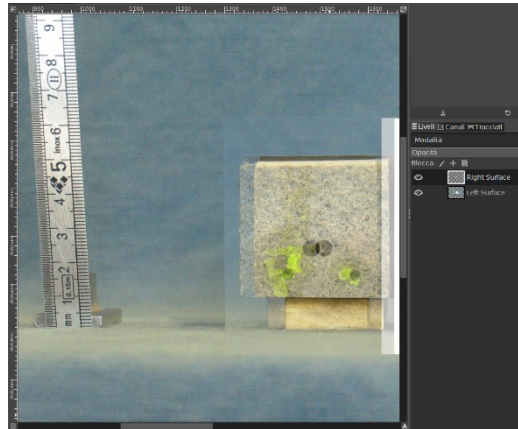


Figure 3.7. Final overlapping.

- Export of the final copy (**Figure 3.8**):

At this point, all the defects of the photo are correct; thus, the final version of the surface with the healing agent leaked on is completed. Once that only the surface is selected, it is cropped and exported on IMAGEJ.

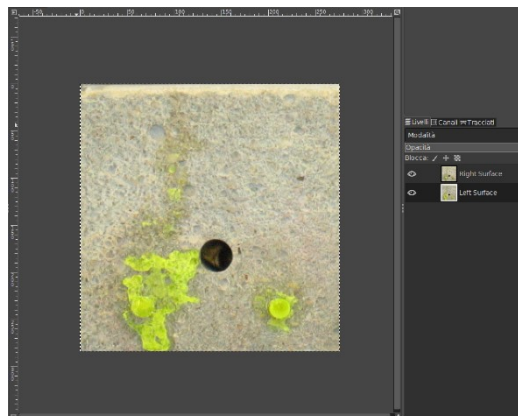


Figure 3.8. Final crop of the image for the export.

3.2. Quantification of the area on IMAGEJ

When the image is finally edited on GIMP, it can be exported on IMAGEJ to be analysed. First of all, it is specified that the software used was IMAGEJ- v. FIJI; in detail, FIJI is an image processing package with a lot of plugins which facilitate scientific image analysis [15]. In this phase, the area is individuated by the software with a research based on the pixel analysis; after this step, the percentage of area covered by the healing agent is finally defined.

In this case, the starting point is the image with the overlapped surfaces, exported from GIMP. Exactly as done before, the procedure provides different steps that consist in:

- Segmentation of the image (**Figure 3.9**):

this represents the most important step of all the procedure: the aim is to determine the components of the image through the examination of its pixels. This analysis is performed thanks to the *plugin Trainable Weka Segmentation*. By definition, it combines machine learning algorithms with examples provided by the user for a predicting modelling [15]; actually, it is considered a versatile tool for this kind of approach [16]. Practically, the user has to define a classifier which is made up of not more of three classes. For each of them, a series of infinitesimal areas must be specified by the user to declare which pixels the various sections are composed of. Training the classifier, it will learn how to segment the image. As final result, the plugin returns a probability map of all the classes: in this way, the image has been separated into its components (healing agent/matrix) automatically. It is evident that the definition of the classes, in terms of manual selection of the areolas, depends on the discretion of the user; this makes the segmentation highly conditioned by the operator's sensitivity.

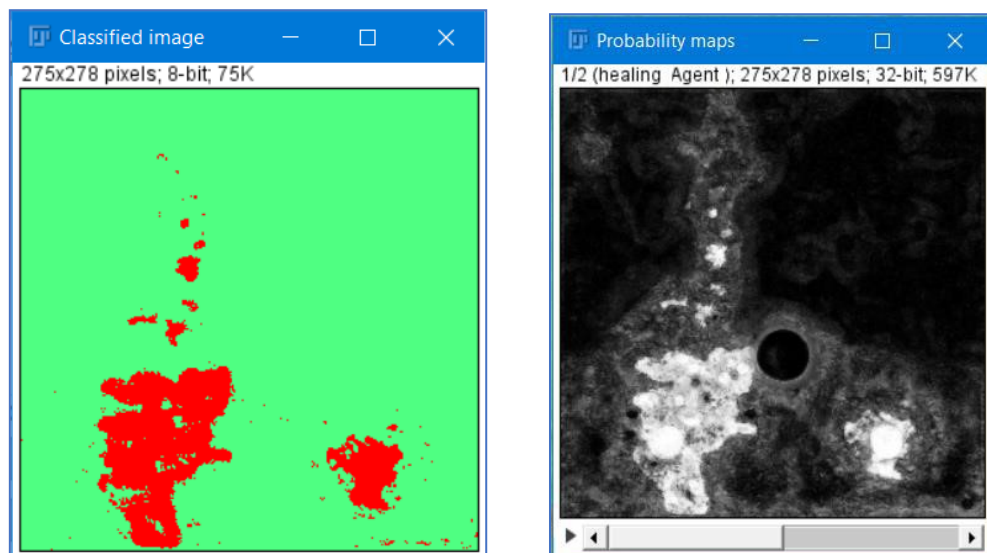


Figure 3.9. Classification and probability map returned by the plugin.

- Bilinearization of the selection (**Figure 3.10**):

the probability map of the healing agent is now converted in a black and white image, through the *Command Binary*; in order to avoid wrong application of a threshold the user needs to select the Default one. Essentially, the thresholding technique divides the image in its foreground and background part by choosing a value cut-off [15].

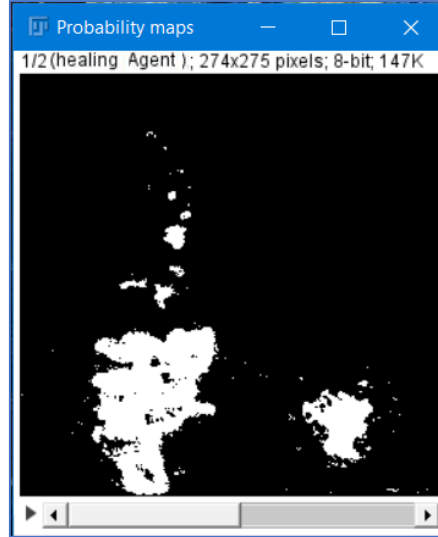


Figure 3.10. Application of the thresholding technique to the probability map.

- Removal outliers (**Figure 3.11**):

despite of an accurate segmentation, errors during the classification of the image are unavoidable. Thus, the removal of the outliers is another important procedure in the analysis. It consists in two steps: the first one allows the elimination of the pixels in excess from the boundaries of the objects with the *Command Erode*; the second one removes the elements that exceed the superimposed threshold, that is expressed in form of radius of the objects, respect to the median of the pixels in the surrounding with the *Command Remove outliers* [15]. Usually, this is an iterative procedure.

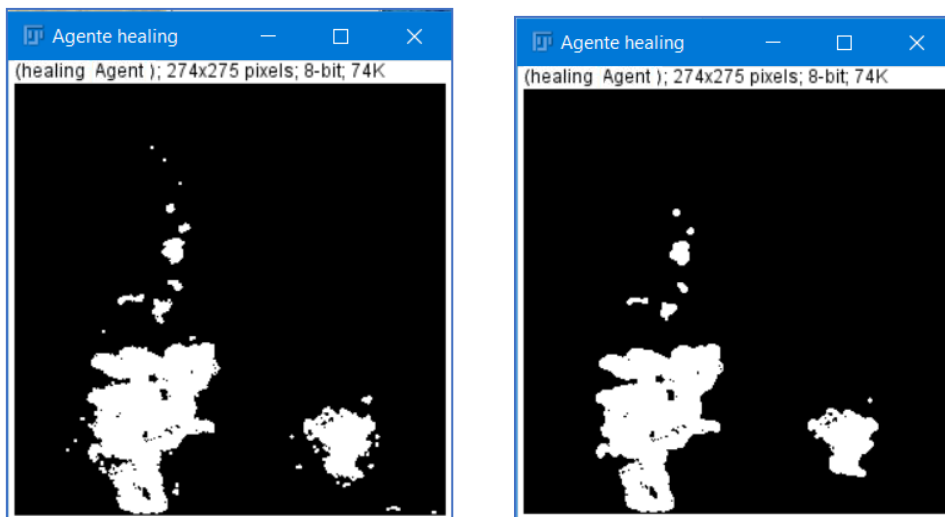


Figure 3.11. Two steps to remove outliers from the final image.

- Calculation of the area in [pixels]:

now that the bilinearized image is free from errors it means that it is made up only of the pixels that really constitute the healing agent class. Thus, it is possible to examine the histogram of the image to find out how many white pixels the foreground is made of and how many black pixels the background is made of. It is evident that the value of area is now expressed in pixels.

- Conversion of the value in [mm²]:

considering that the value of area expressed in pixels is not very indicative, it is converted in square millimetres. As discussed in the *Paragraph 3.1*, the adopted reference quantity is the width of the specimen. Thus, knowing that the conversion factor amounts to 7.125 pixels/mm, the converting expression consists in the Equation (7):

$$\text{Area healing agent (in sq. mm)} = \frac{\text{Area healing agent (in pixels)}}{\text{conversion factor}^2} \quad (7)$$

Usually, this quantity is expressed as percentage of the total covered area of the specimen, according the Equation (8):

$$\% \text{Total covered Area} = \frac{\text{Area healing agent (in sq. mm)}}{\text{Total area}} * 100 \quad (8)$$

where

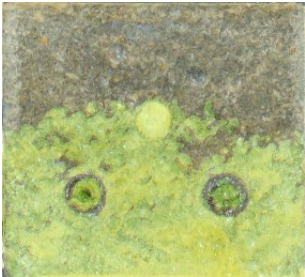



Total area is the area of the surface of fracture, supposed ideally square. The area is calculated including also the surface covered by the capsules and the hole; in detail, for the specimens that have a notch for the pre-cracking test, the area is defined net of its dimensions.




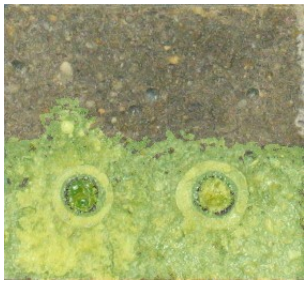

The values of area of the healing agent, calculated according this procedure, are reported in the *Paragraph 3.3*. It contains also the images of the spreading regions identified by the plugin of IMAGEJ. Note that for the series RRT5 a double segmentation is attached in form of case (a) and (b); this comes from an uncertain evaluation of the covered area. It means that, looking at the surfaces, they present a sort of halo that surrounds the polyurethane. The halo could signify that in that area the healing agent was present after the break of the capsules but which was then absorbed by the matrix; in this case, it






would be ineffective on the sealing of the crack so it is excluded from the calculation of the spreading area: this is the case (b). The other hypothesis is that the area occupied by the halo was really invaded by polyurethane but which has accidentally come off the surfaces when the specimens were handled after the complete failure; in this case, the polyurethane is considered active for the sealing so it is included in the calculation of the spreading area: this is the case (a).






In any case, for all the analysis, the values of the case (a) will be used; thus, in the following paragraphs the case (a) will be easily called RRT5.






3.3. Final results






Series	Sample		Spreading area of the healing agent [mm ²]	Area respect to the total area [%]
A_CAP	1		749	52.1
A_CAP	2		847	58.8
A_CAP	3		872	60.6
A_CAP	4		715	49.7






A_CAP	5		765	53.1
A_CAP	6		824	57.2
B_CAP	1		954	66.3
B_CAP	2		735	51.1
B_CAP	3		910	63.2

B_CAP	4		788	54.7
B_CAP	5		871	60.5
B_CAP	6		291	20.2
RRT5 case (a)	1		1086	67.8
RRT5 case (a)	2		929	58.1

RRT5 case (a)	3		827	51.7
RRT5 case (a)	4		524	32.8
RRT5 case (a)	5		537	33.6
RRT5 case (a)	6		301	18.8
RRT5 case (b)	1		673	42.1

RRT5 case (b)	2		240	15.0
RRT5 case (b)	3		549	34.3
RRT5 case (b)	4		164	10.2
RRT5 case (b)	5		182	11.4
RRT5 case (b)	6		133	8.3

CCAP_S	1		21	1.3
CCAP_S	2		42	2.7
CCAP_S	3		80	5.0
CCAP_S	4		18	1.2
CCAP_S	5		27	1.7

CCAP_L	1		136	8.5
CCAP_L	2		277	17.3
CCAP_L	3		303	18.9
CCAP_L	4		120	7.6
CCAP_L	5		228	14.2

CCAP_L	6		195	12.2
--------	---	---	-----	------

Looking at the images, the series RRT5, CCAP_S and CCAP_L show the presence of open pathways. Obviously, they allowed the transit of the water through them during the permeability tests; however, this aspect will be studied in deep in *Chapter 4*. It is evident that configurations of the healing agent like these do not guarantee an excellent protection of the system from the exterior. Also the absent contact of the polyurethane leaked at the height of the two capsules does not contribute to the creation of a barrier against water pressure, as happened for the samples of the series CCAP_S and RRT5.

Moreover, the geometry of the specimens A_CAP and B_CAP certainly promoted the sealing of the hole; in fact, these are the series with the capsules placed closest to the hole. Also its sealing improves unavoidably the recovery of durability properties. In general, as it will be described in *Chapter 4*, even just the sealing of the surface surrounding the hole is enough to reduce the passage of water. In fact, this is the case of some samples of RRT5: they did not show a complete filling of the hole, only a partial one, but for them better results were recorded in terms of water flow than the rest of the series.

Finally, considering the typology of polyurethane used, it was confirmed a greater spreading and amount of leaked agent for the series A_CAP and B_CAP, being the sealant more expansive than that used for the rest of the series. A not comparable percentage of spreading between series CCAP_S and CCAP_L was measured, despite the capsules contained the same quantity of healing agent.

3.4. Considerations and drawbacks

The results of the paragraph 3.3. are now summarized in **Figure 3.12**. in terms of average surface coverage (%) of the healing agent on the crack faces for each series.

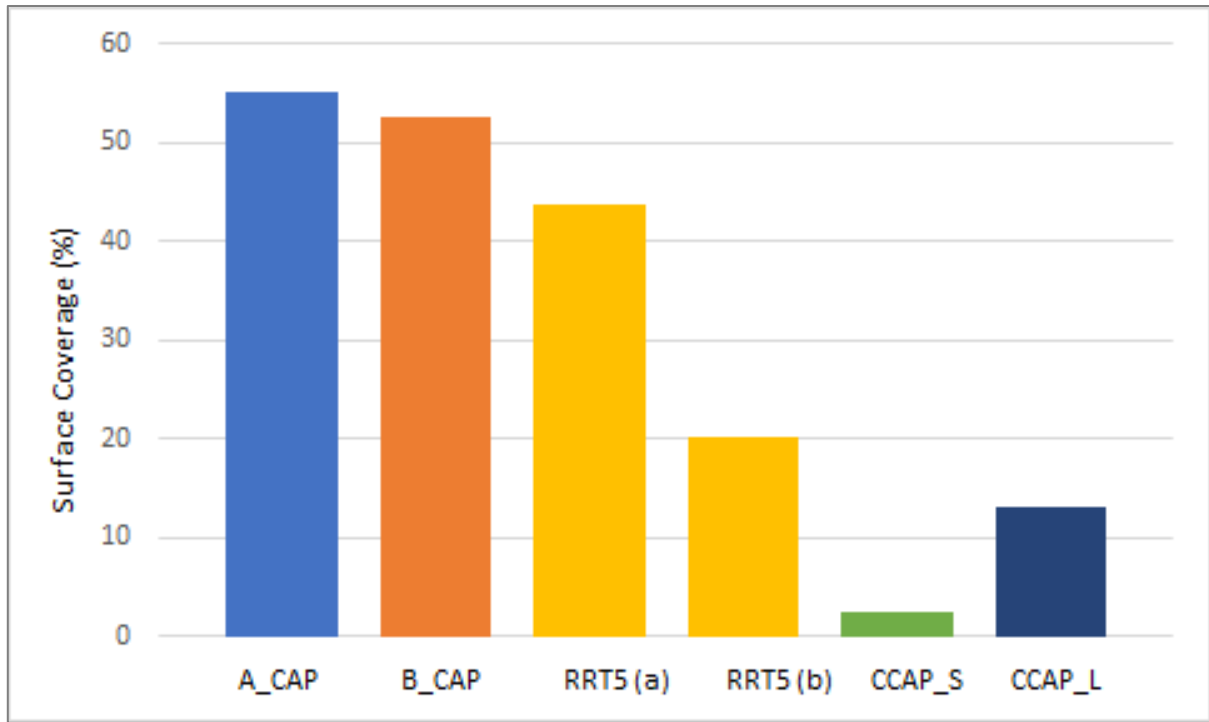


Figure 3.12. Percentages of covered areas by the healing agent for each series.

Analysing the images of the spreading regions, it is evident that for almost all of the specimens the part of crack faces covered by the healing agent is the bottom part, above the crack mouth. In reality, series RRT5 shows a good spreading also in the upper part of the surface. Regarding the mechanism of spreading, it is important to notice that the area of the agent must be a continuum, that is isolated quantities of agent are physically impossible. For this reason, if they are present, it means that part of the sealant has been absorbed by the matrix. Moreover, in this analysis the following assumption is made: if a part of the crack face is covered by the healing agent, it means that also the specular part on the other face was covered by it though any sign is actually present; it is assumed that after the separation the sealant has completely detached itself from one face remaining only on the other one. Thus, the segmentation of the graphically overlapped surfaces represents an automatic way to realize the “OR” of the spreading regions. In general, the satisfactory spreading comes from the use of the polyurethane and its precursors. In fact, in most of the cases, it was also able to fill the cavity left by the holes, when present. Another sign that the sealing of the crack surface was optimal is the foam visible on the samples’ edges, already during the pre-cracking stage, for the series A_CAP and B_CAP.

Definitely, the quantification of the spreading area is an analysis that can be simply performed at the end of all tests, to measure the percentage of area covered by the healing agent. It is a non-invasive measurement and it does not require advanced equipment (only a digital camera).

As anticipated before and as better developed in *Chapter 4*, the quantification of these areas has minor meaning without a correlation with other parameters. Moreover, the accuracy of the results is not less important. In fact, it is evident that the segmentation phase is highly conditioned by the user's discretion, although the selection of the reference areas of each component is precise. Anyway, a research in this sense is often done in several studies [3], [5], [9] for its recognized validity.

4. Relations between tests results and spreading areas

The calculation of the surface coverage allows the expression of the spreading area of the healing agent by numbers; in this way, it represents not only a qualitative parameter but also a quantitative one. In fact, the importance of its evaluation depends by the possibility to express a correlation with other quantities. For the self-healing systems, it is evident that a regression is researched with the recovery indices of the mechanical tests or with the results of the durability ones. In reality, high attention is reserved also to the geometry of the spreading area, in terms of spatial distribution or, for example, moment of inertia. In this paragraph, all these regressions are reported, in order to explain and compare the achieved results.

4.1. Correlation between Water Flow and surface coverage

Figure 4.1. shows the values of water flow of each specimen for all the series in function of the calculated spreading areas.

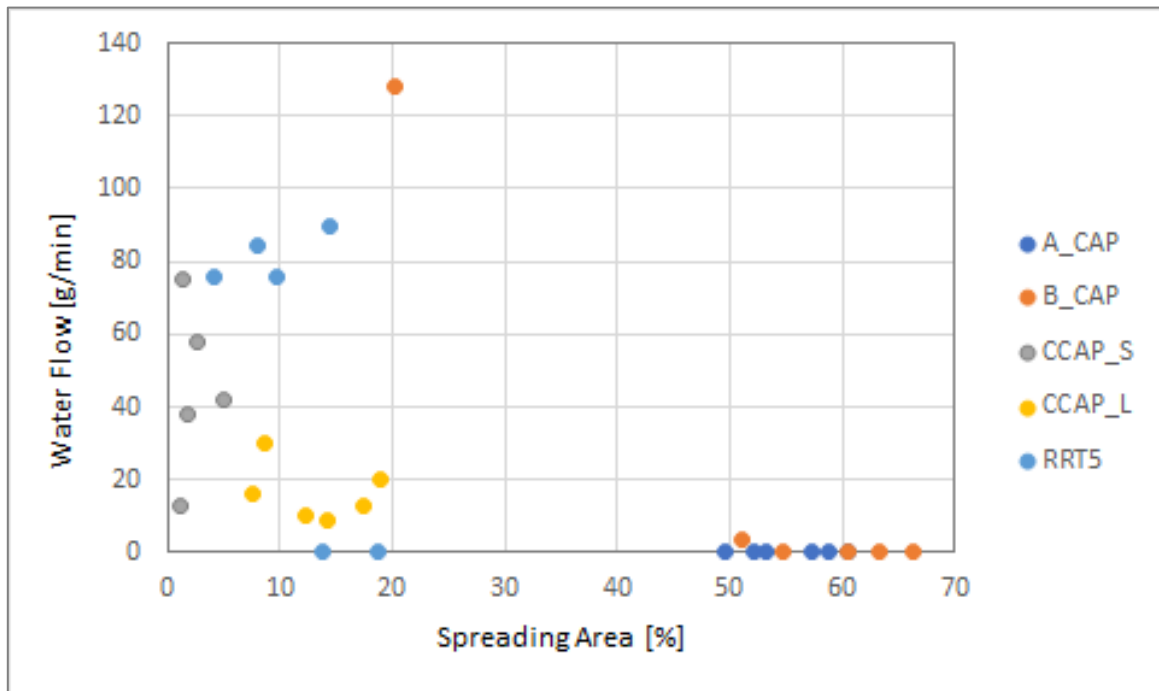


Figure 4.1. Correlation between Water Flow and Spreading area for specimens of the series A_CAP, B_CAP, RRT5, CCAP_S, CCAP_L.

Looking at the graph, it is evident that the specimens that have reached the higher level of spreading of the healing agent show good results in the water flow test, namely the amount of

passed water is absolutely negligible. In detail, the best recovery in terms of durability was registered for B_CAP, except for only one of its samples that, as already discussed in *Paragraph 2.3.2.2*, has been excluded from the analysis for its statistical inconsistency. Moreover, this is also the series with the highest percentage of calculated covered area. Good results also for A_CAP in terms of water flow and spreading area. Different behaviour was shown by the series CCAP_L and CCAP_S. In fact, they present the lowest evaluation of spreading area but, on the contrary, acceptable results in the water flow test. Thus, considering the observations done before, this could seem a nonsense. In reality, this is a clear explanation of how the correlation of area value with its geometrical properties is fundamental. In fact, in the water flow test, the distribution of the healing agent conditions strongly the transition of the water through the crack. This means that, despite of the registration of a high spreading area, if the crack mouth or, when present, the cast-in hole has not been sealed, the water will cross the specimen, causing insufficient results in terms of durability recovery. In this case, no samples of the series CCAP_L show the filling of the hole and, above all, the spreading of the healing agent affected the lateral areas and the part above the capsules, leaving the lower central part partially uncovered. Regarding CCAP_S, it showed the worst results in terms of spreading; in fact, it was also the series with the highest water flows. A similar behaviour to CCAP_L was found for the series RRT5. In fact, also these specimens did not get a filling of the central hole and, in general, a coverage of the later part of the crack faces. In fact, non-zero values of water flow have a single physical meaning: open passages for water. However, the sealing of the surface surrounding the hole was enough to prevent the water flow; it is the case of the samples RRT5_1 and RRT5_3. Despite this, the results achieved with the water flow test are acceptable.

So, to conclude: RRT5 and CCAP_S are the series with the same geometry and amount of stored agent but with a different material for shells; definitively, they showed comparable water flow results, with the exception of two samples of RRT5 that have not showed any flow. The series CCAP_S and CCAP_L are comparable for the amount of agent but stored in a different number of capsules. In this case, the series with the biggest diameter (CCAP_L) showed better results in terms of permeability recovery. Finally, the series A_CAP and B_CAP are practically identical for geometry and materials, except for the absence of the hole for B_CAP. In fact, its absence leads to the comparison of test results of unidirectional and bidirectional flows respectively. Both cases showed a total closure of the cracks. These results are particularly significant for the series B_CAP because it is evident that they confirm a perfect sealing of the interior.

It is also important to underline that what also makes the results of the different series comparable is having guaranteed a constant pressure during the test; this means having create a constant driving force for all.

In view of what has been said, the excellent results in durability recovery of A_CAP and B_CAP are ascribable to the perfect sealing of both hole and crack mouth, not to the high spreading in general. Definitely, a strong relation between the durability recovery and the surface coverage cannot be expressed. In fact, the variation of the results underlines that they are function of the distribution of the agent which itself depends on the complex mechanism of self-healing. The path that the spatial disposition of the healing agent grants to water is what really needs to be evaluated; thus, the distribution of the healing agent respect to the position of the crack mouth and the cast-in hole must be analysed.

4.2. Evaluation of the moment of inertia of the spreading areas

As further parameter, it is now discussed the evaluation of the moments of inertia of the spreading regions of the healing agent. The description of the used method for the calculation of the inertia precedes some considerations about the importance of its estimation.

For this evaluation, the starting point is the segmented binary image of the healing agent obtained on IMAGEJ; this is imported on MatLab and it is converted in a logical array. Thus, the defined array is made up of $i \times j$ elements, which are equal to 0 if they correspond to black pixels while they are equal to 1 if they correspond to white pixels.

Because the surface has an irregular geometry, the moment of inertia has to be calculated per steps, starting from the discretization of the area in infinitesimal ones. In fact, the idea is to define the moment of inertia I with the expression (9):

$$I = \sum_{i=1}^{row\ size} A_i y_i^2 \quad (9)$$

Where, as also explained in **Figure 4.2**,

- the index i is defined from 1 to the row size;
- A_i is area of all the white elements that constitute the row- i ;
- y_i is the distance between the barycentric axis of the transversal section (considered plain) of the specimen and the row- i ; the choice of the barycentric axis is a hypothesis

which has the objective of making these results comparable with those obtained by applying the most widely used Beam theory. It is evident that this is an ideal theoretical assumption, since the hypotheses of validity of the mentioned theory are not satisfied. The idea is to guarantee a continuity for the comparison with other results.

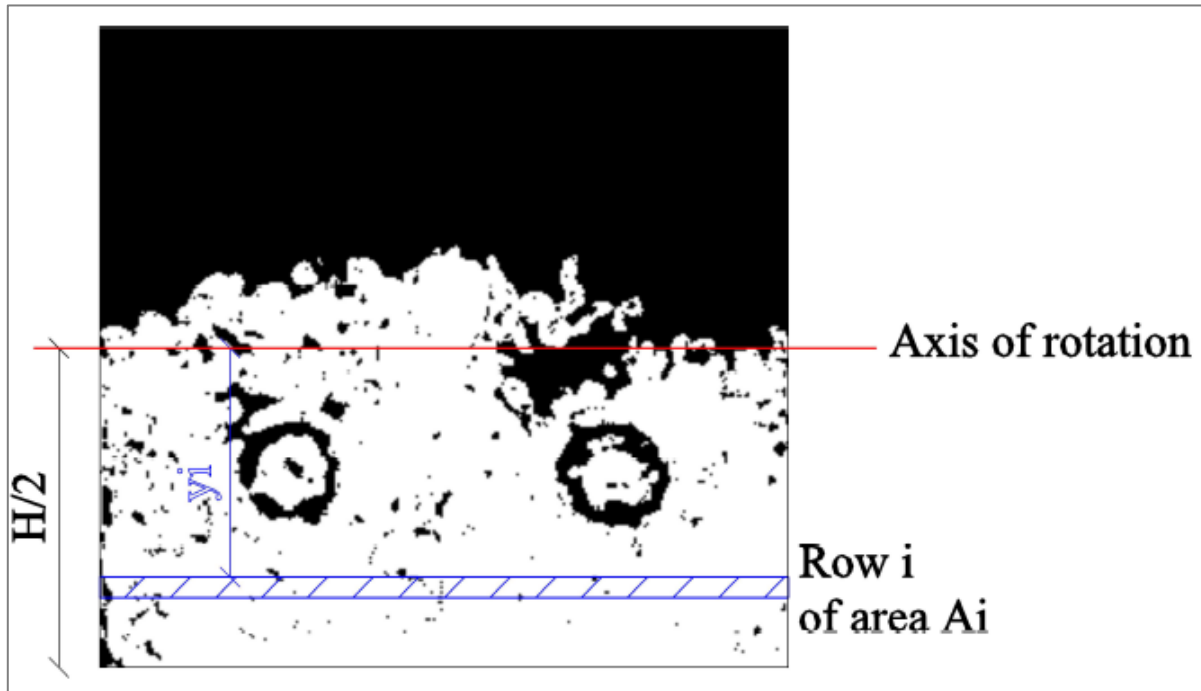


Figure 4.2. Example of calculation of the moment of inertia.

As anticipated before, the moment of inertia is calculated respect to the barycentric axis of the section, considered made up only of mortar. In fact, in the configuration of plain section this axis represents the axis around which the applied bending moment rotates. Implementing the calculation on MatLab, the moments of inertia are calculated for all the specimens; they are reported in **Figure 4.3**.

Series	Sample	Moment of inertia [$\cdot 10^4 \text{ mm}^4$]
A_CAP	1	8.8039
	2	9.0433

4. Correlations between tests results and spreading area

	3	9.5137
	4	8.1569
	5	8.9031
	6	9.3392
B_CAP	1	9.2724
	2	8.0129
	3	8.9912
	4	8.3760
	5	8.7177
	6	0.91317
RRT5	1	18.764
	2	14.491
	3	13.817
	4	9.7401

	5	7.8706
	6	4.136
CCAP_S	1	0.4048
	2	0.9970
	3	1.6085
	4	0.38018
	5	0.5229
CCAP_L	1	3.6836
	2	3.5870
	3	3.8321
	4	2.2573
	5	2.8332
	6	3.2161

Figure 4.3. Moments of inertia of the spreading regions of the healing agent.

Relations between the spreading area and the moments of inertia are reported in **Figure 4.4**.

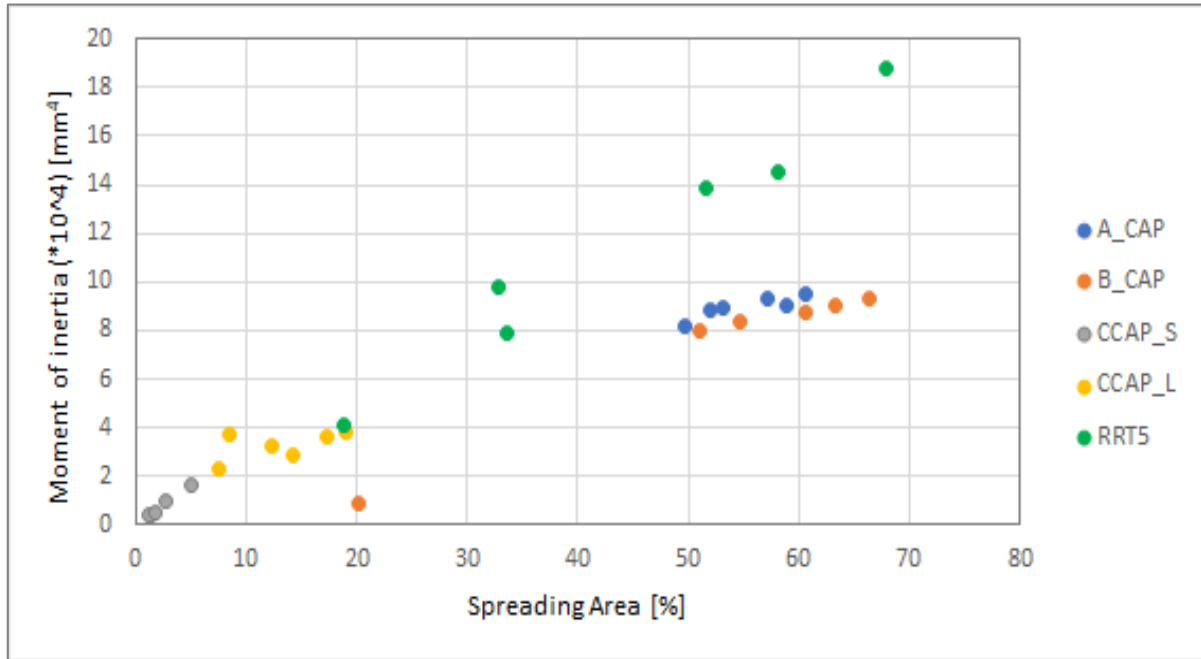


Figure 4.4. Correlation between moments of inertia and spreading regions for all series.

By definition, the moment of inertia represents the geometrical contribution to the flexural rigidity EI of a system [20]. The bending stiffness governs the response to the solicitations according to De Saint Venant Theory. Looking at the expression of the moment of inertia I , its value is directly proportional to the square of the distance of the considered area from the axis of rotation. This means that the higher contribution is provided by the areas that are distributed on the lower or upper part of the crack surface. The best results in terms of inertia were achieved by RRT5; the average moment of inertia is equal to $8.9600 \times 10^4 \text{ mm}^4$. This series, in fact, did not report the highest value of average spreading area but nevertheless it showed above all an overlay of the perimetric parts of the specimen. Good results were registered also for A_CAP and B_CAP; these series show a total coverage of the lower half part of the samples. The series CCAP_L, on the contrary, presents an average moment of inertia of $3.2349 \times 10^4 \text{ mm}^4$ that is about half the value of the previous series; the result remains however optimal considering that its average spreading area is about 13.1%. It follows that the contribution to the moment of inertia comes from the small quantity of agent leaked in the lowest part of the surface and from the choice to place the capsules very close to the bottom edge (3 mm). For the same reason, CCAP_S records a contribution to the moment of inertia instead the slight quantity of polyurethane that has leaked.

Definitely, it is evident that with the same covered area, the contribution at the moment of inertia is greater when the healing agent spreads towards the edges of the crack face.

4.3. Correlation between ILR and surface coverage

This analysis is performed only for the series A_CAP and B_CAP because the reloading test was realized only for these specimens. In this paragraph, the correlation is investigated respect to the evaluated indices of load recovery ILR. The results are summarized in **Figure 4.5**.

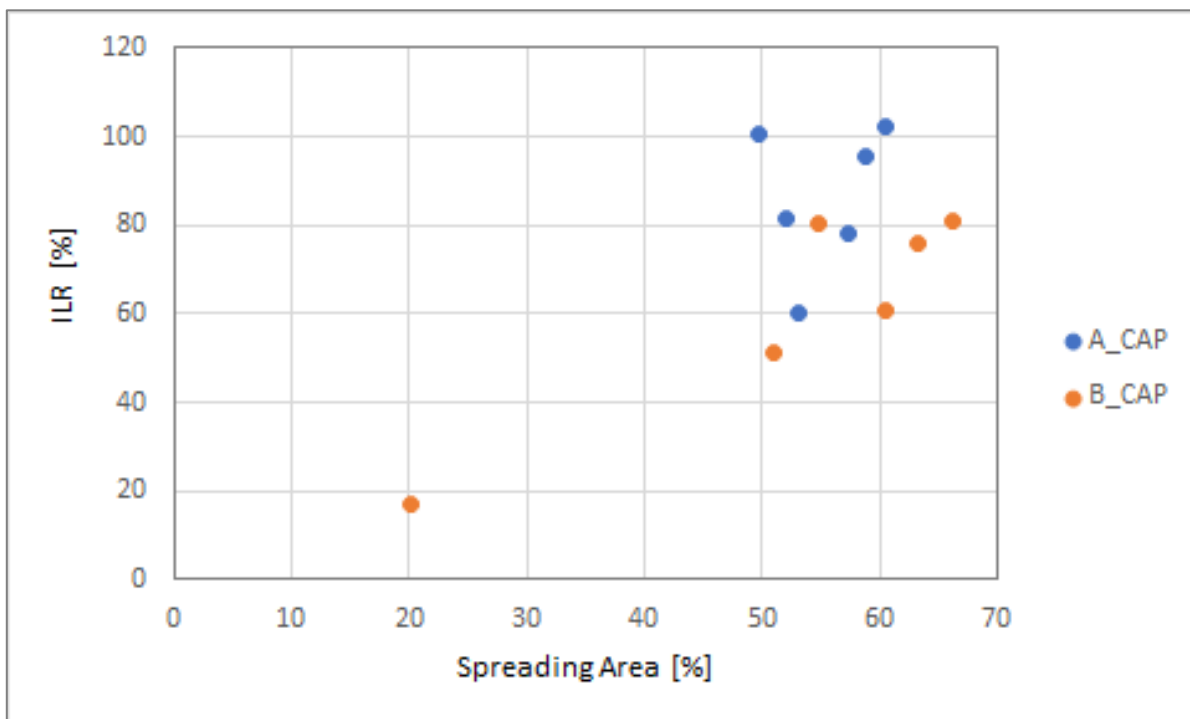


Figure 4.5. Results of reloading tests and spreading areas for A_CAP and B_CAP.

The recovery of the mechanical properties are mainly due to the considerable amount of healing agent that is able to flow into the sample after cracking; in fact, in this case, positive values of ILR have been measured for all the series that show a great spreading of the sealant. In reality, a more complete analysis of this type requires the evaluation of the internal conditions, in order to visualize the diffusion of the agent into the sample. This investigation can be performed realizing a cross section of the specimen in order to study, for example, the amount of sealant solidified inside the capsules or the real position of the capsules inside the sample that determines their different opening during the testing and so a different release of agent. Furthermore, a microscopy investigation allows to identify which parts are solid and which one

are yet liquid; thus, more information about the required curing time for the agent can be extrapolated, as also underlined in other works [10].

Definitely, it was evident that a higher percentage of spreading area would have caused an improvement of the mechanical characteristics because the leaked agent would have been able to react to the stresses, also recreating the continuity of the specimen. Finally, this correlation with the spreading area makes sense considering the ILR value of each sample and not its average value over the series because it is evident that the calculation of the residual load in the pre-cracking test is not easily quantifiable; therefore, separating its value from the single specimen would be incorrect. By definition, in fact, ILR measures the recovery of load capacity net of the residual load at the pre-cracking phase.

Good results for all the series, except for the sample B_CAP_6, that showed the lowest value of spreading area.

4.4. Correlation between IRL and moment of inertia

The correlation between the moment of inertia and the index of load recovery ILR for the series A_CAP and B_CAP is reported in **Figure 4.6**.

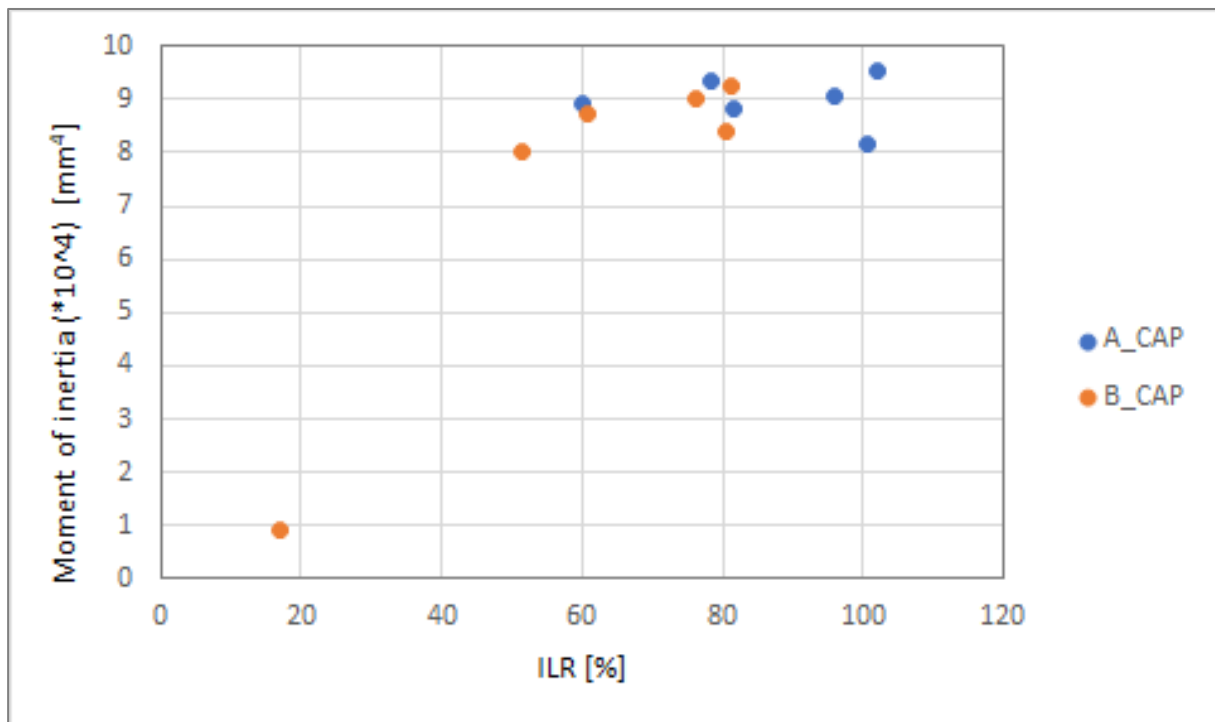


Figure 4.6. Correlation between ILR and their moments of inertia for the series A_CAP and B_CAP.

The obtained results confirm that the greater is the inertia, the greater the mechanical recovery. This is obvious given that the section bending stiffness depends on the EI product. Therefore, considering that for the same material (namely for the same Young modulus value, that in this case it could be both the homogenized one for the polyurethane/cement mortar section and that of the polyurethane if it is assumed that it is the only reactive material after cracking) the bending stiffness is directly proportional to the moment of inertia; thus the greater is the resistance of the section, the greater the recovery of the bearing capacity. As further evidence of what has been said, only the specimen B_CAP_6, with the lowest value of spreading area, showed the lower recovery of load-bearing capacity.

The relation of the spreading area is more significant with IRL indices than with the peak loads of the reloading test because the former represent the true mechanical recovery of the specimen; in fact, they do not take into consideration the residual load from the pre-cracking phase. In this way, the comparison of the spreading regions is with parameters that take into account only the effect of the sealing in the reloading phase.

5. Conclusions and future perspectives

In this work, mortar specimens were produced by incorporating cylindrical macrocapsules and precursors of polyurethane were selected as healing agents from the main types commonly used for self-sealing applications. Five series of specimens were investigated, each one different for composition and coating of the shell, position and dimension of the capsules. Their self-healing efficiency was assessed under permeability and loading tests, namely the durability and mechanical recovery was investigated through water flow test and reloading test respectively. A three-point bending test was proposed to induce a controlled damage but also to evaluate the self-healing effect on the samples up to breaking conditions.

The results highlighted the effectiveness of the investigated systems with regard to their composition, recovery of stiffness, load-carrying capacity, protection from the exterior and spatial distribution of the healing agent. In detail, the choice of cementitious macrocapsules as devices to store the healing agent confirmed their capability to preserve the product and isolate it from the penetration of moisture and other aggressive external agents. Obviously, the highest effectiveness in repairing cracks was shown by the series A_CAP and B_CAP that had the capsules with the larger diameter, that is the capacity to store a greater quantity of sealant. In general, the application of internal and external coating, as well as the blocking of extremes, certainly benefited the preservation of the healing agent, keeping it functional for when the capsules would have been broken by cracks. Interesting, however, was the evaluation of the position of the capsules; their location determines their different opening in the cracking phase, thus a different release of the agent. The highest values of spreading areas were registered for the series A_CAP, B_CAP, RRT5 with the capsules positioned further away from the lower side of the sample, while the remaining series showed a small reversal; in general, the choice of polyurethane was also confirmed effective in terms of conservation and diffusion. The former also recorded an average value of 74% for the LRI in the reloading test, showing a proper recovery of the load-carrying capacity. The evaluation of the spreading regions was realized thanks to the segmentation of the images of the crack faces. The aim of this analysis was the determination of the parts invaded by the agent. In fact, it has been established that what really matters for research is not a generic quantification of the spreading area but its spatial distribution. In fact, it affects the tortuosity of the water path. In general, the series that showed the filling of both the crack mouth and the hole, realized for the execution of the durability test, recorded the lowest water flows; this was the case of the series A_CAP and B_CAP. On the

contrary, the specimens of the series RRT5 manifested a prevalent perimetric distribution of the sealant which did not promote a perfect isolation of the specimen from the external environment but gave it a greater stiffness contribution, if expressed in terms of moment of inertia. Hence, the results highlighted that a direct correlation between the percentage of surface coverage and the durability and mechanical recovery cannot be found. However, it appears that if the healing agent is able to move backward with respect to the direction of propagation of the crack, the recovery turns out to be higher as well as the contribution to the flexural stiffness of the leaked sealant.

Another important aspect that merged from the experimentation was the accuracy to reserve for the casting of the specimens. In fact, as well as taking care of the extrusion of the shells and the moulding of the matrix, their coexistence and compatibility must be carefully pursued. In general, the capsules/matrix contact surface was improved by rolling shells into the sand, contributing positively to the interaction of the components.

Definitely, for all the series encouraging results were achieved regarding the offered protection against the introduction of aggressive agents from the exterior. In this way, the use of these self-healing systems represents an innovative method to increase the service life of the structures. Certainly, further research is needed to complete the detection and the description of these technologies, for example investigating their resistance to freeze-thaw cycles or cyclic loads but, in general, to extreme conditions. Furthermore, the experimentation in full-scale tests and real operating conditions is necessary to really confirm their efficacy. Finally, the definition of guidelines and codes would be helpful; thus, the standardization of the use, production and characterization of self-healing cement-based materials is awaited.

References

- [1] Anglani G., Van Mullem T., Zhu X., Wang J., Antonaci P., De Belie N., Tulliani J.M., Van Tittelboom K. ‘Sealing efficiency of cement-based materials containing extruded cementitious capsules’, *Construction and Building Materials* 251 (2020).
- [2] Formia A., Irico S., Bertola F., Canonico F., Antonaci P., Pugno N., Tulliani J.M. ‘Experimental analysis of self-healing cement-based materials incorporating extruded cementitious hollow tubes’, *Journal of Intelligent Material Systems and Structures* (2016) Vol. 27(19) 2633–2652.
- [3] Ferrara L., Van Mullem T., Cruz Alonso M., Antonaci P., Borg R.P., Cuenca E., Jefferson A., Ng P., Peled A., Roig-Flores M., Sanchez M., Schroefl C., Serna P., Snoeck D., Tulliani J.M., De Belie N. ‘Experimental characterization of the self-healing capacity of cement based materials and its effects on the material performance: A state of the art report by COST Action SARCOS WG2’, *Construction and Building Materials* 167 (2018) 115–142.
- [4] De Belie N., Gruyaert E., Al-Tabbaa A., Antonaci P., Baera C., Bajare D., Darquennes A., Davies R., Ferrara L., Jefferson T., Litina C., Miljevic B., Otlewska A., Ranogajec J., Roig-Flores M., Paine K., Lukowski P., Serna P., Tulliani J.M., Vucetic S., Wang J., Jonkers H.M. ‘A Review of Self-Healing Concrete for Damage Management of Structures’, *Adv. Mater. Interfaces* (2018) 5, 1800074.
- [5] Van Tittelboom K., De Belie N. ‘Self-healing in cementitious materials-a review’, *Materials (Basel)*, 2013 Jun, 6(6): 2182–2217.
- [6] Sánchez M., Faria P., Ferrara L., Horszczaruk E., Jonkers H.M., Kwiecien A., Mosa J., Peled A., Pereira A.S., Snoeck D., Stefanidou M., Stryzewska T., Zają B. ‘External treatments for the preventive repair of existing constructions: A review’, *Construction and Building Materials* 193 (2018) 435–452.
- [7] Anglani G., Antonaci P., Idone G., Tulliani J.M. ‘Self-healing of cementitious materials via embedded macro-capsules’, 4th International Conference on Service Life Design for Infrastructures (SLD4)-27-30 August 2018- Delft, Netherlands.
- [8] Formia A., Terranova S., Antonaci P., Pugno N., Tulliani J.M. ‘Setup of Extruded Cementitious Hollow Tubes as Containing/Releasing Devices in Self-Healing Systems’, *Materials* (2015) 8, 1897-1923; doi:10.3390/ma8041897.
- [9] Anglani G., Antonaci P., Tulliani J.M., Van Tittelboom K., Wang J., De Belie N. ‘Self-

- healing efficiency of cement-based materials containing extruded cementitious hollow tubes filled with bacterial healing agent', Microorganisms-Cementitious Materials Interactions, 25-26 June 2018, Toulouse.
- [10] Anglani G., Antonaci P., Carillo Gonzales S.I., Paganelli G., Tulliani J.M. '3D printed capsules for self-healing concrete applications', 10th International Conference on Fracture Mechanics of Concrete and Concrete Structures, FraMCoS-X, G. Pijaudier-Cabot, P. Grassl and C. La Borderie (Eds), June 2019.
- [11] SARCOS 'Implementing innovative and sustainable solutions for extending the service life of concrete structures', <https://www.sarcos.eng.cam.ac.uk/>.
- [12] CEN 'Methods of testing cement - Part 1: Determination of strength', Ref. No. EN 196-1:2005: E.
- [13] Carpinteri A. 'Scienza delle costruzioni-volume 1', Pitagora Editrice Bologna (1993).
- [14] 'The Free & Open Source Image Editor', <https://www.gimp.org/>.
- [15] 'About ImageJ', <https://imagej.net/ImageJ>.
- [16] Arganda-Carreras I., Kaynig V., Rueden C., Eliceiri K.W., Schindelin J., Cardona A., Seung H.S. 'Trainable Weka Segmentation: a machine learning tool for microscopy pixel classification', *Bioinformatics* (2017) 33(15), 2424–2426.
- [17] Periasamy A., Chang-Ho K., Yu-Jin S., Jae-Seong S. 'Formations of calcium carbonate minerals by bacteria and its multiple applications', *Anbu et al. SpringerPlus* (2016) 5:250, DOI 10.1186/s40064-016-1869-2.
- [18] CEN 'Eurocode 2', Ref. No. EN 1992:2004: E.
- [19] Di Liberto S., Bennardo A., Gabetta G. 'Confronto tra prove in controllo di carico e prove in controllo di deformazione per lo studio della tensocorrosione su acciaio per condotte', da Atti del XIV Convegno Nazionale del Gruppo Italiano Frattura.
- [20] Patela K.A., Bhardwaja A., Chaudharyb S., Nagpalc A.K. 'Explicit expression for effective moment of inertia of RC beams', *Lat. Am. j. solids struct.* vol.12 no.3 Rio de Janeiro Mar. 2015.
- [21] Liao L., Zhang W., Xin Y., Wang H., Zhao Y., Li W. 'Preparation and characterization of microcapsule containing epoxy resin and its self-healing performance of anticorrosion covering material', *Chinese Science Bulletin*, February 2011 Vol.56 No.4-5: 439–443, doi: 10.1007/s11434-010-4133-0.
- [22] Van Mullem T., Gruyaert E., Caspeelee R., De Belie N. 'First Large Scale Application with Self-Healing Concrete in Belgium: Analysis of the Laboratory Control Tests', *Materials* (2020), 13(4), 997, doi:org/10.3390/ma13040997.

- [23] Minova 'Technical data sheet - CarboStop U', TDS_CARBOSTOP U_FEB2019_EMEA_EUR_EN.
- [24] De Neef 'Technical data sheet – HA Flex/Flex LV/Flex SLV AF', 2020 GCP Applied Technologies Inc.